DISSERTATIONES
CHIMICAE
UNIVERSITATIS
TARTUENSIS
155

KADRI LIGI

Characterization and Application of Protein Kinase-Responsive Organic Probes with Triplet-Singlet Energy Transfer

DISSERTATIONES CHIMICAE UNIVERSITATIS TARTUENSIS
155

DISSERTATIONES CHIMICAE UNIVERSITATIS TARTUENSIS
155

KADRI LIGI

Characterization and Application of Protein Kinase-Responsive Organic Probes with Triplet-Singlet Energy Transfer

UNIVERSITY OF TARTU
Press

Institute of Chemistry, Faculty of Science and Technology, University of Tartu

Dissertation was accepted for the commencement of the degree of *Doctor philosophiae* in Chemistry at the University of Tartu on June 30th, 2016 by the Council of Institute of Chemistry, Faculty of Science and Technology, University of Tartu.

Supervisors: Asko Uri, PhD
Institute of Chemistry, University of Tartu, Estonia

Erki Enkvist, PhD
Institute of Chemistry, University of Tartu, Estonia

Opponent: Prof. Niko Hildebrandt
NanoBioPhotonics, Institut d'Electronique Fondamentale, Université Paris-Sud, Université Paris-Saclay, Orsay cedex, France

Commencement: August 22, 2016 at 3.00 PM in room 1021, 14a Ravila St., Institute of Chemistry, University of Tartu

This research has been supported by grants from the Estonian Ministry of Education and Research (SF0180121s08), from Estonian Research Council (former Estonian Science Foundation) (ETF8230, ETF8419, ETF8055, IUT20-17), and from the U.S. National Institutes of Health (R01GM081030); by the Graduate School "Functional Materials and Technologies" receiving funding from the European Regional Development Fund (previously from European Social Fund under project 1.2.0401.09-0079); by European Social Fund's Doctoral Studies and Internationalisation Programme DoRa, which is carried out by Archimedes Foundation; by national scholarship program Kristjan Jaak, which is funded and managed by Archimedes Foundation in collaboration with the Estonian Ministry of Education and Research.

ISSN 1406-0299
ISBN 978-9949-77-195-0 (print)
ISBN 978-9949-77-196-7 (pdf)

University of Tartu Press
www.tyk.ee

CONTENTS

The current thesis is based on the following original publications, referred to in the text by corresponding Roman numerals:

I Vaasa, A.; **Ligi, K.**; Mohandessi, S.; Enkvist, E.; Uri, A.; Miller, L. W. Time-Gated Luminescence Microscopy with Responsive Nonmetal Probes for Mapping Activity of Protein Kinases in Living Cells. *Chem. Commun.* **2012**, *48* (68), 8595–8597

II Kasari, M.; **Ligi, K.**; Williams, J. A. G.; Vaasa, A.; Enkvist, E.; Viht, K.; Pålsson, L. O.; Uri, A. Responsive Microsecond-Lifetime Photoluminescent Probes for Analysis of Protein Kinases and Their Inhibitors. *Biochim. Biophys. Acta - Proteins Proteomics* **2013**, *1834* (7), 1330–1335.

III **Ligi, K.**; Enkvist, E.; Uri, A. Deoxygenation Increases Photoluminescence Lifetime of Protein-Responsive Organic Probes with Triplet–Singlet Resonant Energy Transfer. *J. Phys. Chem. B* **2016**, *120* (22), 4945–4954.

Author's Contribution

I The author participated in planning the experiments and performed the time-lapse images of ARC-Lum(Fluo) probes in live cells and wrote the respective part of the manuscript.

II The author performed the measurements of time-gated luminescence spectra of ARC-Lum probes and participated in the writing of the manuscript.

III The author planned most of the experiments and performed all of the experiments and wrote most of the manuscript. (Compounds applied in the study were synthesized by co-authors.)

ABBREVIATIONS

^1A	ground singlet state of the acceptor-luminophore
$^1A^*$	excited singlet state of the acceptor-luminophore
AF647	fluorescent dye Alexa Fluor 647
AGC	AGC group of protein kinases that is used to define the family of Ser/Thr PKs that are most related to PKA, PKG and PKC
BSA	bovine serum albumine
C	catalase
cAMP	cyclic adenosine 3', 5'-monophosphate
CCD	charge-coupled device
CREB	cAMP response element-binding transcription factor
Cy3B	a cyanine-based fluorescent dye
^1D	ground singlet state of donor-luminophore
$^1D^*$	excited singlet state of donor-luminophore
$^3D^*$	excited triplet state of donor-luminophore
Deox	deoxygenated
DMEM	Dulbecco's Modified Eagle Medium
FRET	Förster resonant energy transfer
FRSK	forskolin, an activator of adenylyl cyclase
G	glucose
GO	glucose oxidase
IBMX	isobutyl-methyl-xanthine, an inhibitor of phosphodiesterases (inhibits PDE1, PDE2, PDE3, PDE4, and PDE5)
IC	internal conversion
ICCD	image-intensified charge-coupled device
ISC	intersystem crossing
K_D	equilibrium dissociation constant determined from the direct binding assay
LED	light emitting diode
MDCKII	Madin Darby canine kidney II cell line
MLC	metal-ligand complex
MSK-1	mitogen and stress stimulated protein kinase 1
NLS	nonlinear least squares
PBS	phosphate-buffered saline
PDE	phosphodiesterase
PF555	fluorescent dye PromoFluor555 structurally resembling the cyanine-based fluorescent dyes
PF647	fluorescent dye PromoFluor647 structurally resembling the cyanine-based fluorescent dyes
Pim-1	protein kinase encoded by an oncogene named proviral integration of Moloney virus 1
PK	protein kinase
PKAc	catalytic subunit of cAMP-dependent protein kinase
PKBγ	γ isoform of protein kinase B (also named as Akt3)

PKCδ	δ isoform of protein kinase C
QY	quantum yield of luminescence
RET	resonant energy transfer
ROCK-II	Rho associated coiled-coil domain containing protein kinase II
S_0	ground singlet state
S_1	first excited singlet state
S_2	second excited singlet state
SEM	standard error of mean
SNR	signal-to-noise ratio
T_1	first excited triplet state
TGL	time-gated luminescence
TMR	fluorescent dye 5-carboxytetramethylrhodamine
TR	time-resolved
TxR	Rhodamine-based fluorescent dye named Texas Red
VR	vibrational relaxation

INTRODUCTION

Protein binding-responsive photoluminescent probes that acquire increased intensity of the luminescence emission in complex with the target protein are in great need for measurement of protein concentration both in biochemical studies and in biomedical research. Because of nanosecond-lifetime autofluorescence of cells and bodily fluids, probes possessing long-lived (microsecond-scale) luminescence emission would allow performance of the measurements in time-resolved (TR) format in a time gate where the fluorescence has ceased.[1,2] Also, by introducing a time-delay into luminescence measurements, signals from probes with microsecond-scale lifetime can be easily distinguished from fluorescent small-molecule compounds and fluorescent proteins used in cellular experiments.[3]

Responsive photoluminescent probes possessing long-lifetime photoluminescence in aqueous solution at room temperature are mostly restricted to lanthanide and noble metal complexes.[4] Although significant improvement has been made in the development of purely organic room-temperature phosphorescent materials within last 5 years, there is still not much known about the application of small-molecule organic phosphors in water solution as most of the research about organic room-temperature phosphorescent materials has been focused to the phosphorescence in solid matrixes.[5] Moreover, small-molecule responsive probes that selectively respond to presence of the analyte have been mostly described for ions and small molecules (pH, oxygen, metal ions, etc.) and probes whose selective binding to target proteins leads to a substantial change in TR signal intensity have been described in rare cases.[6–8]

Novel protein kinase-responsive organic photoluminescent probes [ARC-Lum(Fluo) probes] have been developed in the Institute of Chemistry at the University of Tartu. The association of ARC-Lum(Fluo) probes with a protein kinase (PK) leads to green, yellow, orange or red luminescence with long (microsecond-scale) decay upon illumination with a pulse of near-UV radiation.[9–13] High brightness of the probes is achieved through intramolecular Förster-type resonant energy transfer (FRET) from the excited triplet state of a sulfur or selenium atom comprising heteroaromatic donor-phosphor ($^3D^*$) to singlet state of the acceptor dye (^1A), leading to enhanced emission from the dye. The current study was performed to characterize the FRET-mechanism in ARC-Lum(Fluo) probes; to quantify the microsecond-scale luminescence brightness of the probes and to determine the applicability of the probes for mapping and monitoring the activity of PKs with time-gated luminescence (TGL) microscopy. We now propose a more detailed insight into the photoluminescence phenomenon that is inherent to ARC-Lum(Fluo) probes and describe the application of the probes for TGL measurements. The obtained knowledge can be applied for further improvement of organic probes for analysis of different proteins in biological samples as we have shown to be possible for analysis of PKs.[9,12]

LITERATURE OVERVIEW

1. Photoluminescence

1.1. Fluorescence and Phosphorescence

Research technologies based on the application of photoluminescence (e.g., spectrometry, microscopy, cell sorting) are gaining ever-growing importance in biomedical studies.[14] Therefore, deeper understanding of the physical mechanism behind the phenomenon of photoluminescence can be quickly introduced into successful scientific and technical employment of the phenomenon.

"Luminescence is spontaneous emission of radiation from an electronically or vibrationally excited species not in thermal equilibrium with its environment."[15] Photoluminescence results from the direct photoexcitation of the emitting species: the production of an excited state by the absorption of ultraviolet, visible or infrared radiation. The process of photoexcitation and the following nonradiative and radiative decay can be represented as the Jablonski diagram: a state diagram in which molecular electronic states, represented by horizontal lines displaced vertically to indicate relative energies, are grouped according to multiplicity into horizontally displaced columns. Excitation and relaxation are depicted with arrows, which are generally vertical.[15]

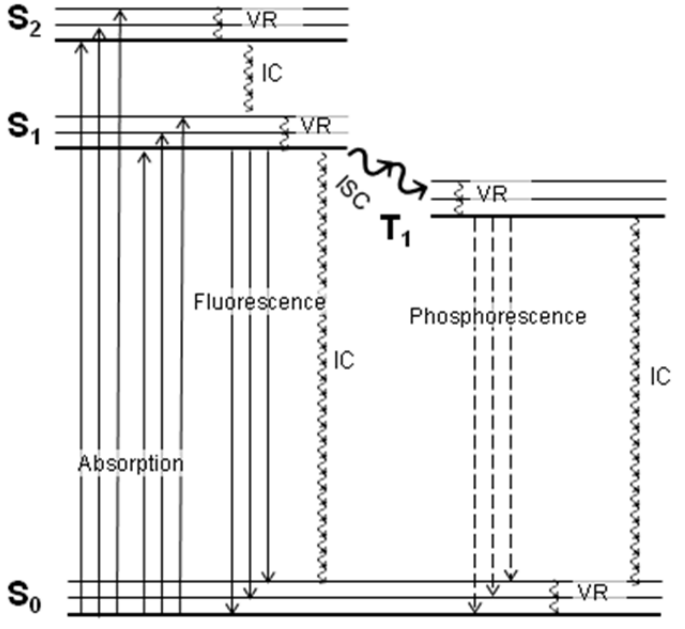

Figure 1. A version of the Jablonski diagram. S_0, ground singlet state; S_1, first excited singlet state; S_2, second excited singlet state; T_1, first excited triplet state; IC, internal conversion; ISC, intersystem crossing; VR, vibrational relaxation

The fragment of the molecule (or atom or group of atoms) in which electronic excitation associated with a given emission band is localized is termed a luminophore. Photoexcitation can lead to the production of two types of the luminophore: fluorophores and phosphors, which either fluoresce or phosphoresce, respectively. Fluorescence emission proceeds predominantly from the lowest vibronic level of the lowest excited singlet state (S_1) of the fluorophore and emission from higher states, e.g., S_2, is not observed. Also, the vibrational levels of S_0 and S_1 are not significantly altered by different electronic distributions of S_0 and S_1. Therefore, the emission spectrum of a fluorophore, which represents radiative decay from S_1 to S_0, is generally the mirror image of the $S_0 \rightarrow S_1$ absorption. Due to rapid thermalization of the excess electronic and vibrational energy (10^{-10}–10^{-15} s) before emission of a photon, the emitted fluorescence has lower frequency than that of the absorbed energy. The corresponding difference of the maxima of the absorption and fluorescence spectra is termed the Stokes shift. The Stokes shift can be further increased by solvent effects, excited-state reactions, association of molecules and/or energy transfer. Also, there is a possibility for intersystem crossing (ISC) into the triplet state, i.e., the electron in the excited orbital can change its spin orientation to be the same as that of the electron that stays in the ground state. The emission resulting from the relaxation of the excited triplet state to ground singlet state is termed phosphorescence. The energy of the lowest vibrational level of the first excited triplet state (T_1) is lower than that of S_1. Furthermore, relaxation from T_1 to S_0 is a spin-forbidden process and therefore occurs on a time-scale much slower than fluorescence. The average luminescence lifetime or decay time (τ), i.e., the average time that the luminophore spends in the excited state before emitting a photon, is typically in the order of nanoseconds (1–10 ns), whereas the phosphorescence lifetime is typically in the range from milliseconds to seconds. The relatively slow radiative decay from T_1 to S_0 if compared to nonradiative deactivation of T_1 causes the very low phosphorescence quantum yields (QYs), i.e., the number of the emitted photons relative to the number of absorbed photons. Therefore, phosphorescence is a rare phenomenon that is usually seen only at low temperatures and highly viscous media (or in solid state). Heavy atoms, e.g., bromine and iodine atoms enhance ISC of the luminophore and thereby increase phosphorescence QY. Both intra- and intermolecular effects of heavy atoms have been described. The phosphorescence QY as well as fluorescence QY can be increased by decrease of temperature that leads to slower nonradiative decay.[15–18]

The distinction between fluorescence and phosphorescence is not always straightforward: transition metal-ligand complexes (MLCs) consisting of a metal and an organic ligand display mixed singlet and triplet states and have luminescence lifetimes in the range of microseconds.[16] Furthermore, the S_1 state can be populated by thermally activated radiationless transition from the first excited triplet state T_1. The process is called E-type delayed fluorescence (also α-delayed fluorescence or α-phosphorescence in older scientific literature). In case of E-type delayed fluorescence, the S_1 and T_1 are in thermal equilibrium and therefore the luminescence lifetime of E-type delayed fluorescence and

phosphorescence are equal. P-type delayed fluorescence occurs in case of triplet-triplet annihilation: $T_1 + T_1 \rightarrow S_1 + S_0$, $S_1 \rightarrow S_0 + h\upsilon$. Another form of delayed fluorescence is recombination fluorescence, which results from the interaction of the S_1 with radical ions of opposite charge or radical ions with electrons. Still, nonradiative decay from T_1 to S_0 is the most common form of T_1 deactivation.[15–18]

1.2. Quenching of Luminescence

The nonradiative decay of an excited luminophore can be enhanced in the vicinity of other molecular entities – quenchers. The term "quenching" is often used in a very broad sense: a process (an energy transfer or a chemical reaction) that leads to the decrease of luminescence emission from the electronic state of the luminophore. For example, ISC from $S_1 \rightarrow T_1$ can also be considered as quenching of the S_1. Quenching has to be distinguished from photobleaching, which denotes the loss of luminescence properties of a luminophore due to an irreversible chemical reaction that dramatically changes the absorption and emission capabilities. In general, two types of quenching occur: collisional or dynamic quenching and static quenching. Sometimes the decrease of luminescence parameters (luminescence lifetime and luminescence QY) with temperature is referred to as thermal quenching. The temperature-sensitivity of luminescence has been taken of advantage for the design of probes and sensors for temperature measurement.[16,18–20]

In case of collisional quenching, the fluorophore is returned to the ground state during diffusive encounter with the quencher and the luminescence lifetime of the luminophore is decreased upon increase of the quencher concentration. Collisional quenching occurs while the luminophore is in the excited state. Hence, the probability of the collision between the quencher and the excited luminophore increases with the luminescence lifetime. Therefore, excited triplet states are more sensitive to collisional quenching than excited singlet states. The best known collisional quenchers are molecular oxygen (triplet oxygen), amines and halogenated compounds. Static quenching occurs if a luminophore forms a nonluminescent complex with the quencher. However, direct physical interaction between the luminophore and the quencher is not necessary to observe static quenching: a long- or short-distance effect can be observed, depending on whether the luminophore is within the interaction area or not. In case of static quenching, the luminescence intensity decreases with number of luminescent entities and the luminescence lifetime does not change.[16,19]

Both static and collisional quenching can be characterized by the Stern-Volmer equation

$$\frac{\Phi^0}{\Phi_q} = \frac{M^0}{M_q} = 1 + K_{SV}[Q] \quad (1),$$

where Φ^0 and M^0 are the quantum yield and emission intensity in the absence of the quencher Q, respectively; Φ_q and M_q are the same quantities in the presence of the different concentrations of Q, respectively, and K_{SV} is the Stern-Volmer coefficient that shows the sensitivity of the luminophore to the quencher. In case of collisional quenching equation 1 can be written as

$$\frac{\Phi^0}{\Phi_q} = \frac{\tau^0}{\tau_q} = 1 + k_q\tau_0[Q] \quad (2),$$

where τ^0 and τ_q are the luminescence lifetimes of the luminophore in the absence and presence of the quencher, respectively and k_q is the bimolecular quenching coefficient that reflects the efficiency of quenching or the accessibility of the fluorophores to the quenchers. The bimolecular quenching coefficient k_q is the product of diffusion-controlled bimolecular quenching coefficient k_0 and the quenching efficiency f_q. Good quenchers like triplet oxygen, acrylamide and iodide ions have quenching efficiencies near unity. Values of k_q smaller than the diffusion-controlled value k_0 can result from steric shielding of the luminophore or low quenching efficiency. Therefore, dynamic quenching can provide information about the internal dynamics of macromolecules, such as proteins.[15,19,21]

In many cases the luminophore can be quenched both by collisions and by complex formation with the same luminophore. Also, the Stern-Volmer relationships are usually not as simple as described by equations 1 and 2. For example, multiple residues of intrinsic luminophore tryptophan (Trp) in proteins are accessed with different efficiency by quencher molecules, such as triplet oxygen, and a more complex mathematical formula have to be used for these cases.[15,19,21]

The phenomenon of quenching has biological applications, e.g., dynamic quenching of long-lifetime luminescence of metalloporphyrins by triplet oxygen is effectively applied for the determination of oxygen concentration in biological samples.[8] A widely applied form of quenching is FRET[22] that enables the determination of the distance between two suitable chromophores, an energy donor and acceptor, separated by 1–10 nm.[23]

1.2.1 Deoxygenation of Aqueous Samples

One critical factor in case of phosphorescence measurements is the quenching of phosphorescence by dissolved molecular oxygen (triplet oxygen). Thus, the relatively low popularity of phosphorescence techniques in the studies on protein structure and dynamics is to a certain extent caused by the existing litera-

ture discrepancy regarding photophysical parameters of the indole luminophore, such as triplet state lifetime, triplet QY and the rate constant for intersystem crossing (ISC).[24] Long history of measurement of protein phosphorescence has shown that improvement of deoxygenation methods leads to increased values of phosphorescence decay time.[25] The most efficient deoxygenation methods require the application of sealed systems, big measurement volumes, extra-purified inert gases, freeze-thaw cycles and other time-consuming procedures that make them not suitable for high-throughput studies.

A two-enzyme method, based on the application of glucose oxidase (GO), catalase and glucose, that effectively generates oxygen deficiency in aqueous solutions, has been in active use for decades. GO catalyses the oxidation of glucose by molecular oxygen and catalase depletes hydrogen peroxide that is produced during oxidation of glucose (Scheme 1). Baumann *et al.*[26] disclosed a simple and efficient variant of the two-enzyme method for generation of oxygen deficiency in cell culture. GO/catalase method enabled quick reduction of molecular oxygen concentration in unsealed vessels. In their unsealed model system without cells the oxygen concentration was decreased by almost 200-fold (down to 1 μM at 37 °C). One drawback of the GO/catalase method is that the added proteins and buffer components can also perform as quenchers for phosphors under investigation.[25]

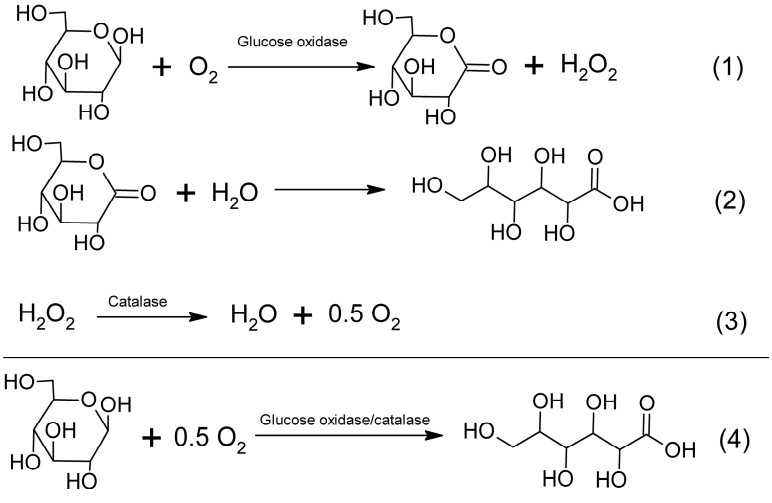

Scheme 1. The GO/catalase method for deoxygenation.[26,27] GO catalyzes the oxidation of D-glucose by molecular oxygen (1). The formed D-gluconolactone rapidly reacts with water to produce D-gluconic acid (2). The hydrogen peroxide is decomposed in the presence of catalase (3). The net reaction is the production of D-gluconic acid by oxidation of glucose (4).

1.3. Resonant Energy Transfer

Resonant energy transfer (RET), also known as electronic energy transfer (EET), is a form of nonradiative energy transfer whereby an electronically excited donor-luminophore transfers its excitation energy (intra- or intermolecularly) to an acceptor chromophore.[28,29] RET is a long-range (usually 1–10 nm) dipolar interaction between two molecular entities.[29] Hence, RET occurs at distances comparable to the dimensions of most biomolecules.[22,29,30] Also, RET makes possible measurement of luminescence intensities at two different wavelengths (both the donor and the acceptor emission or excitation intensities are determined), which makes the measurement ratiometric. Ratiometric measurement regime reduces the disturbing environmental effects and variations in probe concentration and excitation intensity, thereby increasing the reliability of a RET-based assay for characterization of interaction between biomolecules.[31] RET-based probes are widely applied for bioanalytical measurements in different fields of research, both for *in vitro* assays and for *in vivo* monitoring in cellular research.[22,30]

1.3.1. Förster Theory

The theoretical mechanism of resonant energy transfer (RET) was successfully combined with experimental data by Theodor Förster in 1948.[32] In honour of his work the corresponding energy transfer, which follows the distance-dependence in the power of -6 suggested by Förster, is named Förster resonant (resonance) energy transfer (FRET). The formerly used term "fluorescence resonance energy transfer" is considered to be a misnomer.[23] Förster formulated his theory for weak couplings.[23,28] Förster theory can be applied for the characterization of RET between singlet and triplet states of the luminophores and also from triplet to singlet state.[33] In the latter case, the slow rate of the energy transfer from T_1 to S_0 is compensated by the long luminescence lifetime of T_1.[17,34]

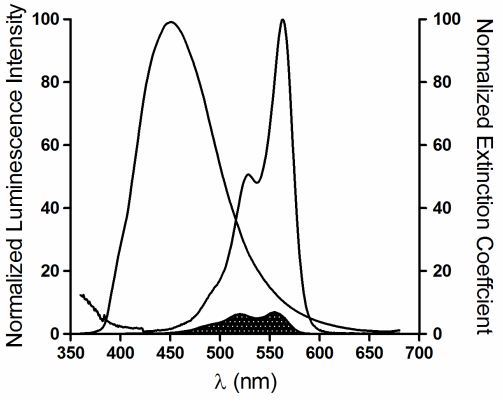

Figure 2. The spectral overlap integral (dotted black area) of the luminescence emission spectrum (left) and absorption spectrum (right) of the donor and the acceptor, respectively.[29]

An important requirement of FRET is that there must be at least a partial spectral overlap between the luminescence emission spectrum of a donor and the absorption spectrum of the acceptor: the donor must be a luminophore, but the acceptor can be a luminophore or a nonemitting chromophore (Figure 2).[29]

The bigger the spectral overlap integral (equation 3), the longer the distance at which FRET can occur. The spectral overlap integral can be calculated by the equation (3)[35]

$$J(\lambda) = \frac{\int_0^\infty F_D(\lambda)\varepsilon_A(\lambda)\lambda^4 d\lambda}{\int_0^\infty F_D(\lambda)d\lambda} \quad (3),$$

where $J(\lambda)$ is the spectral overlap integral; ε_A is the molar extinction coefficient of the acceptor and $F_D(\lambda)$ is the fluorescence emission intensity of the donor in the wavelength range $\lambda+\Delta\lambda$. The spectral overlap integral can then be applied to calculate the Förster distance (the Förster radius) R_0 for a given donor-acceptor pair in known environment by the equation (4)[35,36]

$$R_0 = 0.02108\left(\frac{\kappa^2\phi_D J(\lambda)}{n^4}\right)^{\frac{1}{6}} \quad (4),$$

where R_0 is the Förster distance in the units of nm; κ is the orientation factor in the power of 2; Φ_D is the quantum yield of the donor luminescence in absence of the acceptor; n is the refractive index of the solution (1.33 for aqueous solutions); $J(\lambda)$ is the spectral overlap integral calculated by equation 3 and 0.02108 is the coefficient that can be applied if the extinction coefficient and wavelength is expressed in units of $M^{-1}cm^{-1}$ and nm, respectively. The orientation factor for a given donor-acceptor pair depends on the direction of the emission transition moment of the donor ($\vec{\mu}_D$) and the absorption transition moment of the acceptor ($\vec{\mu}_A$), and the line $\vec{R}$ connecting the centers of the donor and the acceptor (Figure 3) as described by the equation (5)[28,36]

$$\kappa = \vec{\mu}_D\vec{\mu}_A - 3\left(\vec{\mu}_D\vec{R}\right)\left(\vec{\mu}_A\vec{R}\right) = 2cos\theta_D cos\theta_A + sin\theta_D sin\theta_A cos\varphi \quad (5),$$

where φ is the angle between $\vec{\mu}_D$ and $\vec{\mu}_A$ on a plane perpendicular to $\vec{R}$; θ_D is the angle between $\vec{\mu}_D$ and $\vec{R}$ and $\theta_A$is the angle between $\vec{\mu}_A$ and $\vec{R}$.

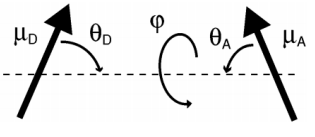

Figure 3. Definitions of the angles used for calculating the orientation factor between two dipoles. The figure has been presented in its original form.[28]

κ^2 can vary between 0 and 4, corresponding to perpendicular and collinear/ parallel positioning of the interacting chromophores, respectively.[22,37] In case the orientations of the donor and acceptor dipoles randomize within the lifetime of the donor excited state, the system is in the dynamic averaging regime and in these isotropic conditions the κ^2 equals to 2/3.[36] The assumption of isotropic conditions is justified if chromophores are bound to polypeptides and proteins.[23,38] However, this assumption may not be valid in case the chromophore forms strong chemical bonds with the polypeptide.

The Förster distance calculated by the equation 4 for a FRET pair in certain conditions determines the FRET efficiency E at the distance R between the donor and the acceptor. If R is equal to the Förster distance R_0, the rate constant of the energy transfer k_{FRET} is equal to the rate constant of the decay of the excited donor in the absence of the energy transfer (k_D), *i.e.*, the processes are equally probable and FRET efficiency equals to 0.5:

$$k_{FRET} = k_D \left(\frac{R_0}{R}\right)^6 = \frac{1}{\tau_D}\left(\frac{R_0}{R}\right)^6 \quad (6),$$

$$E = \frac{k_{FRET}}{k_{FRET}+\tau_D{}^{-1}} \quad (7),$$

where τ_D is the donor luminescence lifetime in the absence of the energy transfer. It is clear from equations 6 and 7 that the efficiency of FRET (E), which is the ratio of k_{FRET} and the sum of all rate constants that contribute to the decay of the excited donor, is dependent on the R/R_0 ratio in the power of -6:

$$E = \frac{1}{1+\left(\frac{R}{R_0}\right)^6} \quad (8).$$

FRET efficiency can also be determined by acceptor sensitization (increase of emission of acceptor at the excitation wavelength of the donor) as well as by donor quenching, which causes the decrease of luminescence lifetime and luminescence intensity of the donor:

$$E = \frac{\varepsilon_A}{\varepsilon_D}\left(\frac{I_{AD}}{I_A} - 1\right) f_D \quad (9),$$

$$E = 1 - \frac{\tau_{DA}}{\tau_D} = 1 - \frac{I_{DA}}{I_D} \quad (10),$$

where E is FRET efficiency; ε_A and ε_D are the molar extinction coefficients of the acceptor and donor at the excitation wavelength of the donor, respectively; I_{AD} and I_A are the fluorescence intensities of the acceptor in the absence and presence of the donor, respectively; f_D is the fractional labelling of the donor; τ_{DA} and I_{DA} are the luminescence lifetime and luminescence intensity of the donor in presence of the acceptor, respectively, and τ_D and I_D are the lumines-

cence lifetime and luminescence intensity of the donor in absence of the acceptor, respectively.[23,36,39]

The FRET efficiency E and the Förster distance R_0 can then be applied for the determination of the distance R between the donor and acceptor:

$$R = R_0 \left(\frac{1}{E} - 1\right)^{\frac{1}{6}} \quad (11).$$

The sensitivity of the FRET efficiency to the donor-acceptor distance is most prominent in a region between $0.5R_0$ and $2.0R_0$, i.e., if $0.015 < E < 0.98$ (Figure 4). Therefore, care must be taken when choosing the right donor-acceptor pair for studying the molecular interaction of interest.[36]

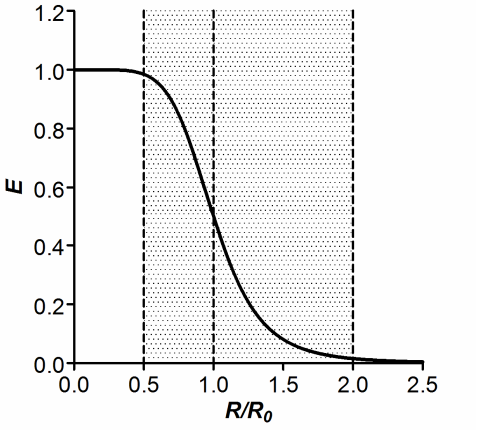

Figure 4. Dependency of FRET efficiency on the R_0-relative distance between the donor and the acceptor chromophores (equation 8).[37]

1.3.2. FRET-Based Probes for Bioanalytical Methods

The chromophores suitable for FRET-based bioanalytical analysis can be divided into various classes: organic materials (including small-molecule probes as well as polymers), materials including an inorganic component (e.g., MLCs, gold nanoparticles), fluorophores of biological origin (intrinsic fluorophores and fluorescent proteins) and biological compounds that exhibit bioluminescence upon enzymatic catalysis.[22] The most common molecules applied in the design of FRET-based probes are small-molecule organic fluorophores, such as cyanine dyes and rhodamine dyes.[22] Here again, the acceptor does not have to be fluorescent (a dark quencher) for FRET to occur. Several FRET-based molecular beacons employ the latter combination of the chromophores to achieve the change in the intensity of the luminescence signal as the result of binding to a

nucleic acid.[22,40] The principal advantage of a dark quencher is that it makes possible the monitoring of the donor channel alone without the interfering signal from the acceptor.[22] On the other hand, this approach to the construction of FRET-based probes loses the possibility to perform the measurements in a ratiometric format.

Another possibility for improving the sensitivity of a FRET system is separating donor emission from that of the acceptor emission in the time-domain by application of a donor with long luminescence lifetime ($\tau > 100$ ns) together with a TR measurement system (Figure 5).[22,41] The approach also decreases the signal of autofluorescence, thereby increasing the sensitivity of the FRET system.[22,41,42] The most common long-lifetime probes applied in biophysical research are MLCs, which include complexes of lanthanide ions, such as Eu^{3+} and Tb^{3+}.[22] Lanthanide-based probes allow the measurement of distances longer than 10 nm.[22,41] However, this may also become a disadvantage if the molecular interaction of interest occurs at much shorter distances (Figure 4).[43] The advantages of lanthanide-based probes also include multiple distinct, sharp emission bands, large Stokes shifts and insensitivity to triplet oxygen.[22,41,44] The peculiarity of lanthanide luminescence is that it is unpolarized and if applied as a FRET donor, the averaging condition $\kappa^2 = 2/3$ becomes a good approximation in several biosensing applications.[42] Luminescence lifetimes of lanthanide-based probes range from microseconds to milliseconds[45] and therefore inexpensive light sources with rather long afterglow, such as flash lamps, are suitable for excitation of lanthanide-based probes.[22,44–46] In comparison to lanthanide-based probes, transition metal complexes have luminescence lifetimes shorter than 100 μs and can be applied in luminescence polarization assays.[45,47] The downsides of MLCs are the multistep synthesis and the possibility of dissociation and/or ligand exchange, which is of utmost trouble for *in vivo* applications and restricts the choice of chelating molecules.[45] Therefore, organic probes with long-luminescence lifetime would be useful for *in vivo* applications. Unfortunately, purely organic luminophores with long luminescence lifetime that would be applicable in a biosensing assay are not common as most of the research about organic room-temperature phosphorescent materials has been focused on the phosphorescence in solid matrixes.[5] Hence, there is still not much known about the application of small-molecule organic phosphors in water solution.

1.3.3. ARC-Lum(Fluo) Probes

In 2011 we reported novel organic photoluminescent probes (ARC-Lum probes) that upon binding to a PK emitted light with long (microsecond-scale) luminescence decay time after illumination of the complex with a pulse of near-UV radiation.[9–13] ARC-Lum probes can be divided into two categories. Firstly, ARC-Lum(-) probes are structurally conjugates of adenosine analogues and peptides (ARCs) that incorporate a heteroaromatic bicyclic or a tricyclic fragment with a sulfur or a selenium atom in one of the aromatic rings. The hetero-

aromatic and peptidic moieties are tethered by a chiral spacer and one or two linkers. The heteroaromatic fragment of an ARC-Lum(-) probe targets the ATP-binding pocket of the PK, where it possesses phosphorescence emission at 450–750 nm upon excitation with a pulse of near-UV radiation. Additionally, ARC-Lum(-) probes possess weak fluorescence emission at wavelength range from 400 to 600 nm. Secondly, ARC-Lum(Fluo) probes are FRET-based tandem probes that in addition to the donor-phosphor of ARC-Lum(-) probes incorporate a fluorescent dye (e.g., HiLyte 488, TMR, Cy3B, TxR, and AF647) whose absorption spectrum at least partly overlaps with phosphorescence emission spectrum of the sulfur or selenium atom-comprising heteroaromatic fragment. Upon binding to a PK and excitation with a pulse of near-UV radiation ARC-Lum(Fluo) probes emit light with microsecond-scale luminescence decay time (τ = 20–250 µs in the presence of dissolved molecular oxygen), therewith the luminescence emission spectra of the probe coincides with the fluorescence emission spectrum of the attached dye.[9,11,13]

A cascade mechanism of energy transfer that was proposed for the discovered phenomenon included FRET from $^3D^*$ of the low-QY donor-phosphor to ^1A possessing high QY.[9] This energy transfer leads to the excited singlet state of the acceptor ($^1A^*$), which thereafter emits light, resulting in powerful sensitisation of the phosphorescence emission.[9] Long lifetime of the emission mediated by the short-lifetime fluorescent dye is due to slow resonant energy transfer from $^3D^*$ to ^1A leading to excitation of the dye to $^1A^*$ and relaxation of $^3D^*$ to the ground singlet state ($^3D^* + {}^1A \rightarrow {}^1D + {}^1A^*$). In case the efficiency of ISC as well as the efficiency of FRET is 100%, the QY of microsecond-scale luminescence is that of the acceptor.[48–50]

The amplification of a microsecond-lifetime luminescence signal of the donor-luminophore by a conjugated organic fluorophore leading to long-wavelength long-lifetime tandem dyes has been described for metal-ligand complexes conjugated with organic dyes (MLCs).[48–51] The amplification of phosphorescence signal of an organic phosphor by a conjugated fluorescent dye resulting from triplet-singlet energy transfer at room temperature in aqueous solution was first described by us for ARC-Lum(Fluo) probes.[9]

The discovered binding-responsiveness of luminescence intensity of ARC-Lum probes could be reasoned by restricted molecular movements of the heteroaromatic phosphor if the probe is associated with the ATP-binding pocket of the PK, but also with decreased quenching rates of the heteroaromatic fragment by dissolved molecular oxygen and buffer components. Therefore, one aim of the current thesis was the establishment of the impact of dissolved molecular oxygen on the microsecond-scale luminescence decay times of both free and PK-bound probes. It was proposed that the dissolved molecular oxygen rapidly quenched the $^3D^*$ of free ARC-Lum probes whereas the diffusion of oxygen was slower into the catalytic pocket of a PK, thereby increasing the QY of $^3D^*$ upon binding to a PK. The second question that was addressed within the project, was the possibility of energy transfer from $^1D^*$ to ^1A. If there is energy transfer from $^1D^*$ to ^1A, it would contribute to the depopulation of $^1D^*$ and may

decrease efficiency of ISC, that would thereby lead to the reduction of intensity of microsecond-scale luminescence of ARC-Lum(Fluo) probes.

ARC-Lum probes have been successfully applied in binding and displacement assays and also in live cell experiments.[9,11] The microsecond-scale luminescence lifetime of ARC-Lum probes enables to differentiate the long-lifetime signal from autofluorescence of the biological samples as well as from the nanosecond-scale fluorescence emitted by the acceptor. As a part of this project it was shown that the luminescence of ARC-Lum(Fluo) probes can be detected in live cells by application of TGL microscopy.[12]

1.4. Measurement of Luminescence

Luminescence measurements can be performed in steady-state or TR measurement mode.[16] In case of steady-state systems, the emission intensity is detected while the sample is being illuminated with a continuous beam of light.[16] Due to the nanosecond-lifetime of fluorescence, the steady-state, *i.e.*, the state of constant emission intensity, is reached almost immediately.[16] In contrast to steady-state measurements, a pulsed excitation is applied for TR luminescence methods to measure the intensity decay of the sample.[16] Most of the measurement systems of fluorescence are steady-state measurements, however, with the rapid decrease of price of instrumentation, the TR measurement systems have gained more popularity.[16,52] In contrast to TR methods, steady-state measurement systems are all intensity-based. Although different ratiometric approaches have been introduced to reduce the susceptibility of intensity-based measurements to inaccuracies caused by variations in luminophore concentration and inhomogeneity, the sources of error are not completely eliminated.[53] The TR measurement systems of luminescence lifetime are concentration-independent and a more sensitive alternative to steady-state measurements for the detection of molecular interactions.[16,52,53] Furthermore, TR methods provide more information about the flexibility of a (bio)molecule.[16,54]

1.4.1. Time-Resolved Measurement of Luminescence

TR luminescence spectroscopy can be divided into two technologies for measuring luminescence decay times: time-domain and frequency-domain measurements.[37,52,55] Frequency-domain methods use intensity-modulated light.[37,55] Typically sinusoidal modulation of light is applied.[37,55] The emitted light will follow this modulation frequency, but with a time delay.[37] The luminescence decay time(s) can be determined from the phase shift or the modulation ratio.[37] Usually, a range of frequencies is applied together with the nonlinear leastsquares (NLS) fittings of the phase or demodulation response.[53] In case of time-domain measurements the luminescence intensity of the sample following the excitation pulse is detected and the NLS analysis is applied for the determination of the luminescence decay time(s).[37,53] The pulse width of excitation light

that is applied for time-domain methods is preferably much shorter than the luminescence lifetime of the sample. The interferences from autofluorescence and scattering that introduce a short-lived optical component into the signal, can be easily accounted for in time-domain methods.[53] The correction can be performed either by subtracting the signal from a blank reference or delaying detection of emission until the short-lived components have ceased completely.[53] The reduced background causes the smaller uncertainty of the estimated luminescence lifetime if compared to frequency-domain measurements.[56] However, background suppression by application of pulsed excitation and a time-delay following the excitation pulse have also been demonstrated for the frequency-domain method.[57,58]

The time-domain measurements can be implemented by either application of time-correlated single photon counting (TCSPC) or the time-gated detection of luminescence intensity (the stroboscopic method or the pulsed sampling method).[53,55] Due to its high sensitivity and low degree of systematic errors, TCSPC is the preferred method for complex intensity decays; however, for decay times longer than 20 ns, the complexity of a TCSPC is no longer necessary and the time-gated detection is preferred.[55] Time-gated detection can be accomplished by either turning on and off the gain of the detector (the stroboscopic method) or having the detector switched on all the time and measuring the electrical pulse with a sampling oscilloscope.[52,55] The detection gate is displaced across the intensity decay until the entire decay is measured (Figure 5). The time-domain method also enables the acquirement of the integrated signal from light quanta emitted within a specified time window (gate)[53,59] (Figure 5) and hence enables the monitoring of changes of luminescence intensity as the response to various stimuli.

The principles of TGL measurement have been implemented for TGL microscopy. The early TGL microscopes applied mechanical choppers in front of detectors and continuous wave (CW) excitation sources, but these were later replaced with electronically gated devices. Also, conventional charge-coupled devices (CCDs) have been replaced with image-intensified CCDs (ICCDs) or electron-multiplying CCDs (EMCCDs). The light sources suitable for TGL microscopy include flash lamps, lasers and light emitting diodes (LEDs). Flash lamps deliver more energy in the excitation pulse within a shorter time interval compared to chopper-interrupted CW sources. The drawback of flash lamps is their relatively long (up to 50 μs) afterglow following the excitation pulse. LEDs and lasers allow much shorter delay times, leading to enhanced signal-to-noise ratio (SNR): 2 μs long and 10 ns long delay times have been effectively applied for TGL microscopy using a LED or a laser as the excitation source, respectively.[3,46,60]

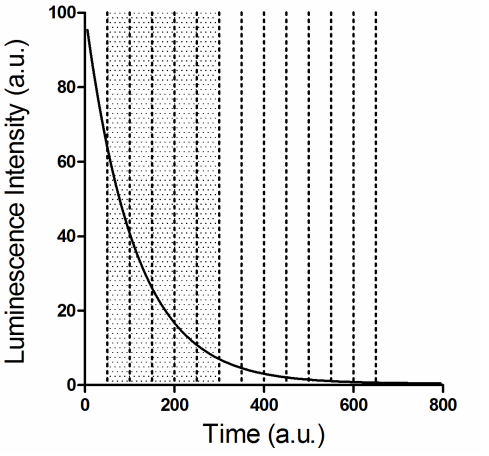

Figure 5. Time-gated measurement of luminescence (TGL measurement). A luminophore emits photons with a characteristic luminescence decay time (solid line). A photon-counting detector sums the number of photons occurring within multiple time intervals (separated with dashed lines). The luminescence intensity emitted within a specified time window (e.g., dotted area on the graph) can be integrated.

2. Protein Kinases

The human kinome comprises 538 genes encoding for PKs. The function of PKs is the catalysis of transfer of the γ-phosphoryl group from a nucleoside triphosphate (NTP) to a target protein/peptide substrate, thereby creating regulatory and recognition sites that influence activity, subcellular localization and other functional characteristics of target proteins. PKs are commonly divided into two types: Ser/Thr PKs and Tyr PKs that transfer the γ-phosphoryl group of a NTP to a Ser, Thr or Tyr residue in the protein substrate, respectively. The catalytic domain of eukaryotic Ser/Thr/Tyr PKs has a bilobal structure. The N-terminal lobe is composed of an antiparallel β-sheet and an α-helix (termed critical α-helix, αC-helix) and the C-terminal lobe comprises α-helices. The two subdomains are joined by a peptide strand (the hinge) with the cleft formed between the subdomains constituting the active site. This cleft has two pockets. The front pocket is involved in either catalysis or NTP binding while the hydrophobic pocket (back pocket) supports regulatory functions.[61]

2.1. Protein Kinases of the AGC Group

Alignment of cDNA sequences of the catalytic PK domain has enabled to divide human PKs into 10 groups.[62] The term AGC PKs is used to define the group of Ser/Thr PKs that are most related to the catalytic subunit of cyclic adenosine monophosphate (cAMP) dependent protein kinase (PKAc), cyclic guanosine monophosphate (cGMP) dependent protein kinase (PKG) and protein

kinase C (PKC).[62] There are 63 PKs in the AGC group and, based on their homology outside the catalytic (kinase) domain, they have been divided into 21 subfamilies.[62,63] They all have a prototypical bilobal kinase fold.[63] 42 of AGC PKs also contain domains other than the PK core, which are involved in regulation of PK activity and localization.[63]

AGC PKs interact with their substrates in many ways. A groove near the active site is involved in substrate binding and determines the sequence specificity of the PK. AGC PKs bind sequences that comprise basic amino acid residues (Arg or Lys) close to the phosphorylation site on the target protein. The consensus motif for target protein consists of 3-7 amino acids.[63]

Enhanced activity of AGC type PKs have been related to cancer, malaria and hypertension;[64–67] hence, PK-responsive probes that enable to study the mechanisms and function of PKs of the AGC group contribute to the search of treatments of these diseases.

2.1.1. cAMP-Dependent Protein Kinase

PKAc belongs to the AGC group of PKs.[62] PKA holoenzyme, tetrameric protein complex comprising two PKAc molecules and a dimer of the regulatory subunits, is the principal intracellular target of cAMP.[68] cAMP/PKAc signaling pathway is known to be regulated by G-protein coupled receptors (GPCRs) that either activate or inhibit the production of cAMP by adenylyl cyclase on the inner membrane surface.[68] Hence, activity of PKA can be regulated by structural analogues of cAMP (e.g., 8-Br-cAMP), effectors of adenylyl cyclase (e.g., forskolin), phosphodiesterases regulating the compartmentalization of cAMP and effectors of GPCRs (e.g., isoproterenol, glucagon, norepinephrine).

PKA holoenzyme is localized to different subcellular compartments through binding to A kinase anchoring proteins (AKAPs).[68,69] Under low levels of cAMP concentration, the holoenzyme is catalytically inactive. When the concentration of cAMP increases, the compound binds to the regulatory subunits of PKA (4 molecules of cAMP per one dimer of the regulatory subunit) causing a conformational change of the protein and the release of two free active catalytic subunits (PKAc-s).[68] Free PKAc can diffuse into the nucleus, where it modifies the functions of a large variety of nuclear proteins, such as cAMP response element-binding transcription factor (CREB) and nuclear factor kappa-light-chain-enhancer of activated B cells (NF-κB).[70]

PKAc is one of the simplest and most studied PKs and is often applied in research as a prototype of PKs.[69] PKAc was used as the model PK within this study.

2.1.2. Labeling of cAMP-Dependent Protein Kinase for Microscopy

Proteins can be labeled chemically or genetically by attaching a luminophore or a fluorescent protein to the protein of interest. Combined technologies have also been developed, e.g., FlAsH and ReAsH tags that are based on a binding reaction between a biarsenical ligand and a genetically encoded tetracysteine motif that has been fused to the target protein.[71,72] The biarsenical ligands emit fluorescence upon binding to the target protein.[71,72] FlAsH tag has been applied for imaging several functional proteins in live mammalian cells including PKAc.[72,73] The main advantage of the FlAsH and ReAsH tags is the small size of the fluorophore.[72] The downsides of the FlAsH/ReAsH technology are the nonspecific labeling of thiol-rich biomolecules and toxicity of the biarsenical ligands and labeling conditions.[72,74,75]

Both subunits of PKA have been successfully labeled with fluorescent proteins.[76] Zaccolo and co-workers designed a DNA-construct, that, when inserted into cells, the corresponding fusion protein could be used to measure the extent of the dissociation of PKA holoenzyme by FRET between the fluorescently labeled regulatory and catalytic subunits.[76,77] The drawback of this method is the overexpression of both subunits that artificially alters both the concentrations and ratio of the regulatory and catalytic subunits of PKA. Also, the additional polypeptide of ~26 kDa (molar mass range of GFP)[78] mass added to the protein may not allow free diffusion of the catalytic subunit (~40 kDa for human PKAc) into the nucleus, because the cutoff between facilitated transport and free diffusion through nuclear pore complex is considered to be ~40 kDa[79]; however, recent studies suggest that bigger proteins can also diffuse into the nucleus.[80,81]

Another possibility for labeling PKA is the application of a small PKA-binding molecule with cell penetrating and luminescent properties. This approach has been applied for labeling PKAc.[12,82,83]

AIMS OF THE STUDY

The general aim of the study was the characterization of photoluminescence of ARC-Lum probes. To achieve this aim, the luminescence brightness and energy transfer efficiencies of ARC-Lum probes had to be determined. In addition, the study had to establish the applicability of ARC-Lum(Fluo) probes in live cells. Several specific tasks were raised within the study:

- recording of TR spectra of ARC-Lum probes;
- determination of QYs of fluorescence and phosphorescence of ARC-Lum probes;
- determination of the impact of dissolved molecular oxygen on the luminescence decay time and luminescence intensity of ARC-Lum probes;
- calculation of Förster distances and FRET efficiencies in ARC-Lum(Fluo) probes;
- calculation of the efficiency of ISC and the QY of microsecond-scale luminescence of ARC-Lum(Fluo) probes and
- application of ARC-Lum(Fluo) probes for mapping and monitoring PKAc activity in live cells as imaged by TGL microscopy.

MATERIALS AND METHODS

Materials

All solvents, buffer components, and referent compounds were obtained from commercial sources and were used as received. The chemicals used for the synthesis of ARC-Lum probes were purchased from Sigma-Aldrich, if not stated differently. Cell culture reagents were purchased from Invitrogen, Inc (Thermo Fisher Scientific). Structures of the ARC-Lum probes applied in the study are shown in Figure 6. (The synthesis of ARC-Lum probes was performed by other group members as described earlier.)[84] The following NHS esters of fluorescent dyes were purchased from commercial resources: TMR (AnaSpec), AF647 (Molecular Probes), PF647 (PromoKine), Cy3B and TxR (GE Healthcare Life Sciences). Concentration of solutions with ARC-Lum probes were determined by UV-vis spectroscopy based on molar extinction coefficient of the luminophore. The molar extinction coefficient ε of ARC-Lum(-) probes ARC-668 and ARC-1138 in a water-based buffer at pH = 7.4 is 15 000 $M^{-1}cm^{-1}$.[9] The molar extinction coefficients that were applied for fluorescent dyes at their absorption maximum were obtained from the provider companies: 130000 $M^{-1}cm^{-1}$ (Cy3B), 85000 $M^{-1}cm^{-1}$(TxR), 80000 $M^{-1}cm^{-1}$ (TMR), 250000 $M^{-1}cm^{-1}$ (AF647 and PF647). The full-length catalytic subunit of human PKA (PKAc) was produced as described previously.[85]

Compound	Type of Compound	X	Y	R
ARC-668	S(-)	S	-	R_1
ARC-669	S(TMR)	S	TMR	R_1
ARC-1134	S(TxR)	S	TxR	R_1
ARC-1182	S(PF647)	S	PF647	R_1
ARC-1085	S(AF647)	S	AF647	R_2
ARC-1086	S(AF647)	S	AF647	R_3
ARC-1138	Se(-)	Se	-	R_1
ARC-1186	Se(Cy3B)	Se	Cy3B	R_1
ARC-1139	Se(PF647)	Se	PF647	R_1
ARC-1144	Se(TMR)	Se	TMR	R_1
ARC-1148	Se(TMR)	Se	TMR	R_4
ARC-1170	Se(PF647)	Se	PF647	R_4
ARC-1185	Se(TxR)	Se	TxR	R_4
ARC-1188	Se(TxR)	Se	TxR	R_5

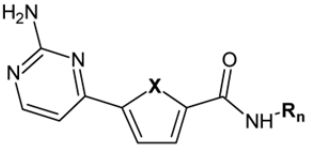

R_1 = Ahx-(D-Arg)-Ahx-(D-Arg)$_6$-[(D-Lys)-**Y**]-NH_2

R_2 = Ahx-(D-Ala)-Ahx-(D-Arg)$_6$-[(D-Lys)-**Y**]-NH_2

R_3 = Ahx-[(D-Lys)-**Y**]-Ahx-(D-Arg)$_2$-NH_2

R_4 = Ahx-(D-Ala)-(D-Arg)$_6$-[(D-Lys)-**Y**]-NH_2

R_5 = Ahx-(L-Ala)-(D-Arg)$_6$-[(D-Lys)-**Y**]-NH_2

Figure 6. Structures of ARC-Lum probes applied for the study. Ahx, 6-aminohexanoic acid moiety; Cy3B, a cyanine-based fluorescent dye; PF647, fluorescent dye PromoFluor647; TxR, fluorescent dye Texas Red

TR Measurement of Luminescence and Deoxygenation of Aqueous Samples

TR measurement of luminescence was performed with four different instruments, which all were operated in time-domain. The photoluminescence spectra of samples with free ARC-1138 in Ar-purged buffer solution or PK-bound ARC-1138 were recorded at room temperature in quartz cuvettes with 10.00 ± 0.01 mm optical path length (Starna Inc.) on a spectrofluorometer (FS900, Edinburgh Instruments) equipped with a photon counting photomultiplier tube (R2658P, Hamamatsu) and using a xenon flash lamp as the excitation source. The TR spectra were recorded with measurement steps of 5 nm on this instrument.

The deoxygenation of samples with argon gas (BOC Gases, Grade 5.5) was monitored on an in-house constructed phosphorometer[86] modified for time-domain operation and equipped with an avalanche photodiode (Hamamatsu), a 365 nm LED, and quartz fibers for the transfer of the excitation radiation to the cuvette.

The TGL spectra of PK-bound ARC-Lum(Fluo) probes were measured at room temperature in a microcuvette (Perkin Elmer) with a spectrofluorometer (Fluoromax-4, Horiba Scientific) as described previously.[11] The time delay and window (integration time) were set to 50 μs and 200 μs, respectively. The components of the buffer (pH = 7.4) were 50 mM Hepes (Sigma, H7637), 150 mM NaCl (Riedel-de Haën, 31434), 0.005% Tween-20 (Sigma, P9416), 0.5 mg/mL bovine serum albumin (BSA, Sigma, A4503) and 5 mM dithiothreitol (Sigma, 43815). No TGL signal was detected for the free ARC-Lum(Fluo) probes in the same conditions.

The temperature dependence of microsecond-scale luminescence lifetime of PK-bound ARC-Lum(Fluo) probe ARC-1186 and free ARC-Lum(-) probe ARC-1138 was studied with a spectrofluorometer (Fluoromax-4, Horiba Scientific) equipped with a fiber optic mount (F4-3000, Horiba Scientific), fiber optic bundles (model 1950, Horiba Scientific) and a temperature-controlled sample compartment (qpod® 2-e, Quantum Northwest). The solution containing GO (2 U/mL) and glucose (25 mM) was applied for the determination of temperature dependence of luminescence decay time of ARC-Lum(-) probe ARC-1138. The same solution containing GO (2 U/mL) and glucose (25 mM) with catalase (120 U/mL) was applied for the determination of temperature dependence of luminescence decay time of PK-bound ARC-Lum(Fluo) probe ARC-1186. The measurements were performed in a sealed quartz cuvette with 10.00 ± 0.01 mm optical path length (Starna Inc.).

The fourth instrument applied for the TR measurement of luminescence was a plate reader (PHERAstar, BMG Labtech.) with appropriate optical modules HTRF802D1 [ex. 330(60), em. 675(50)] or TRF904B1 [ex. 330(60), em. 590(50)]. The measurements were performed on black, low-volume, 384-well, nonbonding-surface microplates (Corning, code 3676) at 30 °C. The assays were performed in phosphate buffer (100 mM sodium phosphate, pH = 7.4) or

Hepes buffer (100 mM, pH = 7.4, Sigma H7637) containing 0.005% Tween-20 (Sigma, P9416) and 0.5 mg/mL BSA (Sigma, A4503). The plates containing samples (15 µL per well) with glucose oxidase (GO, final activity 2 U/mL, Sigma, G6125) and catalase (final concentration 0.05 mg/mL, Sigma, C1345) were pre-incubated at 30 °C for 15 min and thereafter the enzymatic deoxygenation was started by addition of 5 µL of D-glucose (Sigma, G7021) solution (final concentration 25 mM). Two negative controls (one with glucose only and the other with glucose oxidase and catalase) were always monitored if enzymatic deoxygenation was performed. PKAc was always added in small excess to ensure full complexation of the ARC-Lum probe with PKAc. The concentration of the active form of PKAc was determined by titration of the probe using fluorescence anisotropy (FA) or TR luminescence intensity read-out as described previously.[9,11,87] The activity of GO was determined with a porphyrin-based optrode[88] and its performance was measured on the plate reader by monitoring the luminescence lifetime of the oxygen-sensitive probe MX-400 (final dilution 600x, Luxcel Biosciences). The data were analyzed with GraphPad Prism software version 5.0 (GraphPad Software, Inc.).

The microsecond-scale luminescence lifetime of the PK-bound ARC-Lum(-) probe ARC-668 and PK-bound ARC-Lum(Fluo) probes ARC-1085, ARC-1086, ARC-669, ARC-1134, ARC-1170, ARC-1144, ARC-1148, ARC-1185, and ARC-1188 was measured on black low-volume 384-well nonbonding-surface microplates (cat. no. 3676, Corning) with a plate reader (PHERAstar, BMG Labtech). The microplates were incubated for 15 min at 30 °C before each measurement. The samples were made into the assay buffer (pH = 7.4) with 50 mM Hepes (Sigma, H7637), 150 mM NaCl (Riedel-de Haën, 31434), 0.005% Tween-20 (Sigma, P9416), 0.5 mg/mL BSA (Sigma, A4503) and 5 mM dithiothreitol (Sigma, 43815). The TR luminescence intensity was recorded with an appropriate optical module HTRF802D1 [ex. 330(60), em. 675(50)], TRF904B1 [ex. 330(60), em. 590(50)] or TRF1009B1 [ex. 330(50), em. 630(40)] with a 5 µs long measurement step within 800 µs after the excitation pulse. The data were analyzed with GraphPad Prism software version 5.0 (GraphPad Software, Inc.).

Determination of QYs

For the determination of QYs, quartz fluorometric cells with 10.00 ± 0.01 mm optical path length were used (Starna Inc.). The spectra were recorded at room temperature. The one-photon absorption spectra were recorded on a spectrophotometer (Lambda-35 UV-Vis, Perkin Elmer) and steady state fluorescence was measured with the FS900 spectrofluorometer described above. The absorption and the steady-state luminescence spectra were recorded with a measurement step of 1 nm. The maximal number of counts did not exceed 2×10^5 counts-per-second (cps). The excitation energy was corrected for the excitation light intensity measured by the reference detector and the emission signal intensity

was corrected for the wavelength-dependency of the detection system. The emission QYs were determined relative to that of 9,10-diphenylanthracene (DPA) in ethanol (QY = 95%)[89] or Rhodamine 6G (R6G) in ethanol (QY = 95%)[90]. During measurements, the optical density of DPA and R6G was kept below 0.05 units at the absorption maximum. All the dilutions of ARC-Lum probes were made into 50 mM phosphate buffer (pH = 7.4). The refraction indexes used for phosphate buffer, ethanol, and dichloromethane (DCM) were 1.333, 1.361, and 1.424, respectively. The data were processed and the QYs were calculated using the software Origin 7.0 (OriginLab Corporation).

Calculation of Förster Distances and FRET Efficiencies

Förster distances of ARC-Lum(Fluo) probes were calculated on the basis of the overlap of the luminescence emission spectrum of the donor-luminophore and the absorption spectrum of the acceptor-fluorophore by applying equations 3 and 4. FRET efficiency of energy transfer from the triplet state of the donor ($^3D^*$) to the singlet state of the acceptor (^1A) was calculated by equation 10. The efficiency of energy transfer from the singlet state of the donor ($^1D^*$) to ^1A was evaluated by comparison of the normalized steady-state emission spectra of the donor-sensitized acceptor and the acceptor only. Equation 12 was used for the calculation of the efficiency of energy transfer:

$$E = \frac{\varepsilon_A(\lambda_D^{ex})}{\varepsilon_D(\lambda_D^{ex})}\left[\frac{F_{AD}(\lambda_A^{em})}{F_A(\lambda_A^{em})} - 1\right] \quad (12),$$

where E is efficiency of the energy transfer; $\varepsilon_A(\lambda_D^{ex})$ and $\varepsilon_D(\lambda_D^{ex})$ are the molar extinction coefficients of the acceptor and donor at the excitation wavelength of the donor, respectively; $F_{AD}(\lambda_A^{em})$ and $F_A(\lambda_A^{em})$ are the fluorescence intensities of the acceptor in the absence and presence of the donor at the emission wavelength of the acceptor, respectively.[37,91]

Binding Assay with TGL Detection

The binding assays were performed according to protocol described previously.[9] Briefly, all biochemical binding experiments were performed on black low-volume 384-well nonbonding-surface microplates (cat. no. 3676, Corning) on a plate reader (PHERAstar, BMG Labtech). The microplates were incubated for 15 min at 30 °C before each measurement. The assay was performed in the buffer solution (pH = 7.4) with 50 mM Hepes (Sigma, H7637), 150 mM NaCl (Riedel-de Haën, 31434), 0.005% Tween-20 (Sigma, P9416), 0.5 mg/mL BSA (Sigma, A4503) and 5 mM dithiothreitol (Sigma, 43815).

To quantify the binding of ARC-Lum probes to PKs, two different binding assays were performed: the titration of the PK with the ARC-Lum probe (termed T1) or the titration of the ARC-Lum probe with the PK (termed T2).

The concentration series of the ARC-Lum probe (T1) or the PK (T2) was made in the assay buffer and the fixed concentration of the PK (5 nM) (T1) or the luminescent probe (2 nM) (T2) was added to each well. The titration of the PK with the ARC-Lum probe (T1) was performed by Dr. Angela Vaasa.

The data from the assays were fitted with the aid of GraphPad Prism software version 5.0 (GraphPad Software, Inc.) and K_D values were calculated using nonlinear regression analysis:

$$TGL = B + M\frac{L_t+K_D+kE_0-\sqrt{(L_t+K_D+kE_0)^2-4L_tkE_0}}{2} \quad (13),$$

where TGL is the detected time-gated luminescence intensity; B is the background signal; M is the luminescence intensity of the PK/ARC-Lum complex at 1 nM concentration; L_t is the total concentration of the ARC-Lum probe; E_0 is the nominal concentration of the kinase; K_D is the dissociation constant between the ARC-Lum probe and PK and k is the fraction of the active kinase.

Cell Culture and Luminescence Microscopy

MDCKII cells were cultured in Dulbecco's Modified Eagle Medium (DMEM) supplemented with 10% fetal bovine serum, 2 mM L-glutamine, 100 U/ml penicillin and 100 mg/ml of streptomycin at 37 °C and 5% CO_2. Cells were passaged using 0.25% trypsin/0.03% EDTA solution. For imaging experiments the cells were trypsinized and reseeded at density of 13 000 cells/well into eight-well chambered slides and incubated at 37 °C and 5% CO_2 overnight (20–28 h).

For endpoint imaging the cells were incubated with 10 μM ARC-1185 or 10 μM TxR-r_9-NH_2 for 1 h at 37 °C, thereafter the cells were washed three times with phosphate-buffered saline (PBS) supplemented with Ca^{2+} and Mg^{2+} ions and then imaged in 100 μL DMEM (free of phenol red) at room temperature. The experiments were repeated at least three times.

For real-time (time-lapse) imaging the cells were washed three times with PBS supplemented with Ca^{2+} and Mg^{2+} ions and then imaged in 100 μL of phenol red free DMEM at room temperature. Thereafter equal volume of ARC-1185 or ARC-1188 (20 μM in DMEM) solution containing (or not containing) forskolin (FRSK, 50 μM) and 1-methyl-3-isobutylxanthine (IBMX, 200 μM) was added to the cells to obtain the incubation solution containing ARC-1185 or ARC-1188 (10 μM), FRSK (25 μM or missing) and IBMX (100 μM or missing). The images were taken at the following timepoints: 1, 3, 5, 10, 15, 20, 30, 45, 60, 75, 90, 105 and 120 min after the addition of ARC-1185.

The cells were imaged using an epifluorescence microscope (Zeiss Axiovert 200) with a 63X/1.25 N.A. EC Plan Neofluar oil-immersion objective (Carl Zeiss, Inc.). For TGL microscopy the microscope was modified with the following components: UV LED emitting at 365 nm (UV-LED-365, Prizmatix); delay generator (DG645, Stanford Research Systems, Inc.); a gated ICCD

camera and camera controller (Mega-10EX, Stanford Photonics, Inc.) and a computer running Piper Control software (v2.4.05, Stanford Photonics, Inc.). Appropriate excitation source (LED, 365 nm), emission filters [TGL (em. 610(75) nm] and dichroics allowed for wavelength selection. The light source and camera timing parameters were as follows: excitation pulse length, 100 μs; delay time, 10 μs; collection time, 200 μs.

The time-lapse images were analyzed with a ImageJ software version 1.45s (Wayne Rasband, National Institutes of Health, USA). Using ImageJ the luminescence intensity of ARC-Lum/kinase complex per pixel was measured in 9 cells on each image and sets from 3 experiments were averaged. Distinction was made between the luminescence intensity change in the cytoplasm and in the nucleus. The background was defined as the area with no cells on the image and it was measured in four different locations on the image. The datasets were then analyzed with GraphPad Prism software version 5.0 (GraphPad Software, Inc.)

For steady-state fluorescence microscopy, the epifluorescence microscope was equipped with a 100 W mercury arc lamp for excitation and appropriate filter cube [FL (ex. 545(30) nm, em. 605(15) nm] for wavelength selection. The ICCD camera was set to automatic gain level and acquisition time.

RESULTS AND DISCUSSION

1. Photoluminescence of ARC-Lum Probes (Papers II, III, and Unpublished Data)

1.1. Absorption and Luminescence Spectra of ARC-Lum(-) Probes

ARC-Lum probes used in the current study comprise either a thiophene- or a selenophene-containing heteroaromatic luminophore (Figure 6). The probes emit both fluorescence and phosphorescence if illuminated with near-UV radiation. However, the excited triplet state of ARC-Lum(-) probes is quenched by dissolved molecular oxygen and also buffer components (Paper III). Hence, the phosphorescence emission spectra of ARC-Lum(-) probes can be measured either in deoxygenated conditions or if the probe is bound to a PK. Here, ARC-Lum(-) probes containing either the thiophene- or selenophene-comprising luminophore were compared and PKAc was used as the model kinase.

Both the absorption and fluorescence emission spectra of the thiophene-containing probe ARC-668 are blue-shifted compared to the selenophene-containing probe ARC-1138 (Figure 7). Furthermore, the phosphorescence emission spectrum of the luminophore in ARC-668 (data not shown) was also blue-shifted if compared to that of the luminophore in ARC-1138. The phosphorescence emission spectrum of the selenophene-comprising free probe ARC-1138 in deoxygenated buffer solution coincided with that of the PK-bound ARC-1138, which shows that the difference between the energy levels of $^3D^*$ and ^1D in ARC-1138 is not changed upon binding to PKAc.

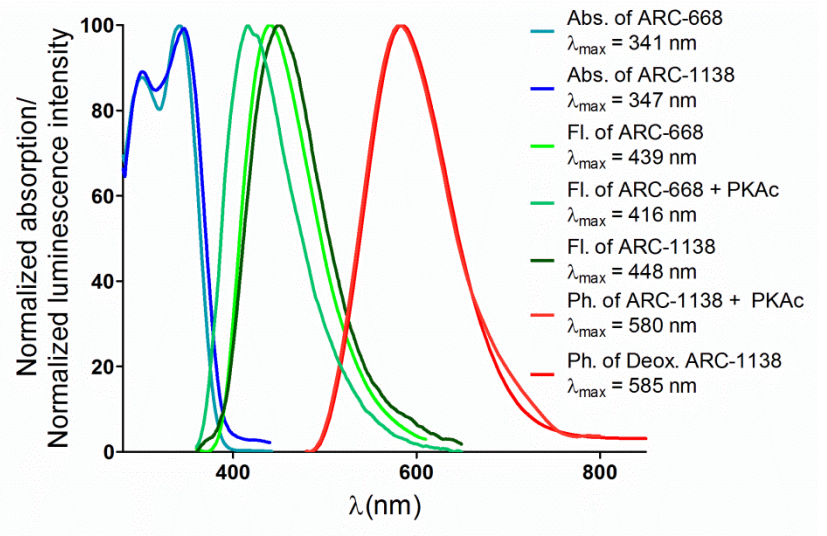

Figure 7. The absorption and luminescence emission spectra of ARC-Lum(-) probes. Abs., absorption spectrum; Deox., deoxygenated; Fl., fluorescence emission spectrum; Ph., phosphorescence emission spectrum

Due to the very low fluorescence QY of ARC-1138, the fluorescence emission spectrum of ARC-1138 in PK-bound state could not be recorded reliably as the measurement would have required concentration of the active kinase above 10 μM. However, the fluorescence emission spectrum of PK-bound ARC-Lum(-) probe could be measured for the thiophene-comprising probe ARC-668 that has fluorescence QY 11-fold higher (Φ = 5.5%) than that of ARC-1138 (Φ = 0.5%).[92] The fluorescence emission spectrum of PK-bound ARC-668 was blue-shifted if compared to the fluorescence emission spectrum of free ARC-668: the maximum of the fluorescence emission spectrum shifted from 439 nm to 416 nm. This blue-shift may be caused by the fixation of the luminophore by the hydrogen bonds formed within the catalytic pocket of PKAc.[93] The blue-shifted fluorescence emission spectrum leads to a smaller spectral overlap between the fluorescence emission spectrum of the donor and that of the acceptor upon binding of the probe to PKAc.

1.2. Time-Gated Luminescence Spectra of ARC-Lum(Fluo) Probes

In addition to a thiophene- or a selenophene-containing heteroaromatic donor-luminophore that is the source of both fluorescence and phosphorescence, ARC-Lum(Fluo) probes comprise an acceptor-fluorophore that commonly is attached to the peptidic moiety in the probe (Figure 6). It was shown in Paper II that the microsecond-scale luminescence excitation spectrum of PK-bound ARC-Lum(Fluo) probes is independent of the acceptor-fluorophore attached to the peptidic moiety, whereas the microsecond-scale luminescence emission spectrum corresponds to that of the acceptor-fluorescent dye. These results supported the mechanism that was previously proposed for the microsecond-scale luminescence of PK-bound ARC-Lum(Fluo) probes, which included FRET from the phosphorescent donor with low QY to the acceptor-fluorophore with high QY ($^3D^* \rightarrow {}^1A$). Also, the phosphorescence emission spectrum of the selenophene-containing $^3D^*$ in PK-bound probe ARC-1138 was very broad and various fluorophores with emission ranging between 550–700 nm could be applied as the acceptor-fluorophore for the $^3D^*$ in ARC-Lum(Fluo) probes, such as TMR, Cy3B, TxR, and PF647 (Figure 8). Furthermore, the phosphorescence emission spectrum of the ARC-Lum(-) probe with benzo[4,5]seleno [3,2-d]pyrimidin-4-one moiety ranged from 440 nm to 600 nm and peaked below 500 nm, enabling in principle the application of acceptor-fluorophores with absorption in the blue, green and yellow regions of the visible spectrum, such as Hylite 488 or fluorescein, but was also applicable as a donor for fluorescent dyes PF555 and PF647.[13]

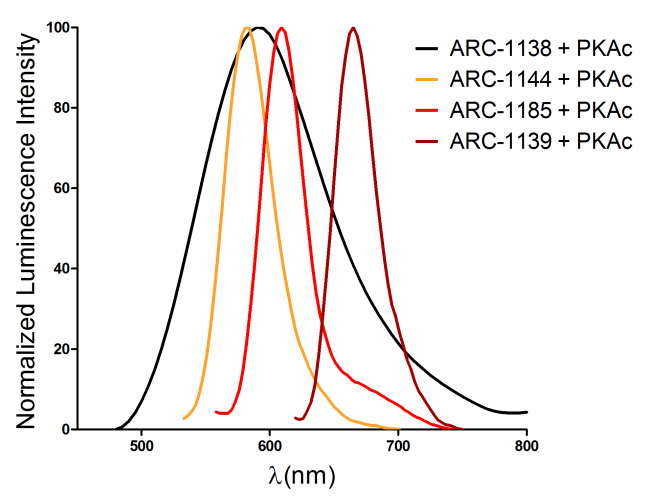

Figure 8. TR emission spectra of PK-bound ARC-Lum probes. The TR spectrum of ARC-Lum(-) probe ARC-1138 was measured with the FS900 instrument (gate 0.2–2 ms) and the TR spectra of ARC-Lum(Fluo) probes with Fluoromax-4 (gate 50–250 μs).

1.3. Oxygen Sensitivity of Luminescence of PK-Bound ARC-Lum Probes

Four ARC-Lum probes were chosen for the study of oxygen sensitivity of PK-bound ARC-Lum probes: the selenophene-comprising ARC-Lum(-) probe ARC-1138 [Se(-)] and three ARC-Lum(Fluo) probes, ARC-1186 [Se(Cy3B)], ARC-1139 [Se(PF647)], and ARC-1182 [S(PF647)]. The deoxygenation of samples was performed at 30 °C by application of the GO-catalase method and the luminescence lifetimes and luminescence intensities were recorded on a plate reader.

Enzymatic deoxygenation of the sample containing ARC-1138/PKAc complex increased luminescence lifetime of PK-bound ARC-1138 [Se(-)] more than 4-fold, from 108 μs to 447 μs (Table 1). The luminescence lifetime of PK-bound ARC-668 [S(-)] could not be determined accurately, however, it is definitely longer than 556 μs, which is the luminescence lifetime of PK-bound probe ARC-1182 [S(PF647)], which includes the thiophene-comprising donor-luminophore as well as the acceptor-fluorophore. The increase of the luminescence lifetime of the donor-luminophore upon enzymatic deoxygenation led to increased efficiency of FRET from $^{3}D^{*}$ to ^{1}A and increased luminescence brightness of the PK-bound ARC-Lum(Fluo) probes ARC-1186 [Se(Cy3B)], ARC-1139 [Se(PF647)], and ARC-1182 [S(PF647)] after deoxygenation. However, the sensitivity of the photoluminescence properties of the PK-bound probes to dissolved molecular oxygen differed for the probes. Thiophene-comprising ARC-Lum(Fluo) probe ARC-1182 possessed the greatest sensitivity: its luminescence lifetime increased from 109 μs to 556 μs (Table 1 and Figure 9). In case of probe ARC-1139, a selenophene-comprising counterpart of probe ARC-1182, the enzymatic deoxygenation increased the luminescence decay

time less than 1.5-fold, from 33 µs to 47 µs. The enzymatic deoxygenation of the sample with PK-bound ARC-1186 led to increase of the luminescence lifetime of ARC-1186 about 2-fold, from 76 µs to 157 µs. These results point to the tendency that ARC-Lum(Fluo) probes with longer decay time possess higher sensitivity to deoxygenation, which is an expected result.

Table 1. Luminescence Decay Times (τ, µs), Normalized Luminescence Intensity (I_0), and Normalized Integrated Luminescence Intensity ($I_0*\tau$) of ARC-Lum Probes in PK-Bound State*

Components added to the probe	**ARC-1138 [Se(-)]**			**ARC-1186 [Se(Cy3B)]**			**ARC-1139 [Se(PF647)]**			**ARC-1182 [S(PF647)]**		
	τ (µs)	***I_0***	***$I_0*\tau$***	***τ (µs)***	***I_0***	***$I_0*\tau$***	***τ (µs)***	***I_0***	***$I_0*\tau$***	***τ (µs)***	***I_0***	***$I_0*\tau$***
+ PKAc + G	111 ± 7	1.0 ± 0.1	1.0 ± 0.1	77 ± 1	28 ± 4.5	19 ± 3	36 ± 3	240 ± 50	77 ± 18	101 ± 4	6.9 ± 0.5	6.3 ± 0.7
+ PKAc + GO + C	108 ± 5	1.0 ± 0.1	1.0 ± 0.1	76 ± 2	37 ± 7.6	26 ± 6	33 ± 1	280 ± 20	83 ± 8	109 ± 5	6.6 ± 0.5	6.4 ± 0.8
+ PKAc + GO + C +G	447 ± 5	1.2 ± 0.1	4.7 ± 0.6	157 ± 4	39 ± 4.2	55 ± 7	47 ± 1	270 ± 33	112 ± 16	556 ± 5	7.5 ± 1.0	37 ± 6

*The data are based on measurements performed with the plate reader PHERAstar at 30 °C in the presence of dissolved molecular oxygen and in enzymatically deoxygenated conditions. The transmittance of the optical filters as well as the concentration of the probe applied for the measurements has been considered for normalization of I_0 of PK-bound ARC-Lum probes. The normalization of I_0 and integrated luminescence intensity ($I_0*\tau$) have been done in relation to ARC-1138/PKAc complex in the presence of dissolved molecular oxygen. Error bars represent SEM (N = 2 to N = 5). GO, glucose oxidase; C, catalase; G, glucose.

The luminescence properties of PK-bound ARC-1186 [Se(Cy3B)] were compared with that of corresponding free probe (Figure 9). In enzymatically deoxygenated conditions the normalized integrated luminescence intensity, i.e., normalized luminescence brightness, $I_0\tau$ (I_0, luminescence intensity extrapolated to t = 0 µs, multiplied with luminescence lifetime τ) of PK-bound ARC-1186 was 30-fold higher than the luminescence brightness of the nonbound probe ARC-1186. This enhancement of luminescence brightness depends on the acceptor-fluorophore conjugated to the donor-luminophore as well as the origin of the PK.[9,13] Due to the differences of luminescence lifetime of the nonbound and PK-bound probe, the binding-responsiveness of ARC-Lum(Fluo) probes could be further increased with the application of the appropriate delay and gate time. For example, in case of gate 150–800 µs, the ratio of PK-bound and free ARC-1186 in enzymatically deoxygenated and nondeoxygenated conditions was 67-fold and 885-fold, respectively.

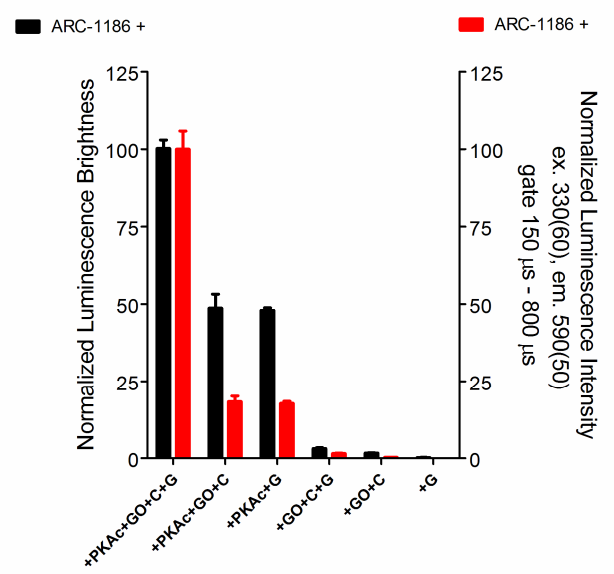

Figure 9. Luminescence brightness ($I_0\tau$) and luminescence intensity (gate 150–800 µs) of ARC-1186 [Se(Cy3B)] in PK-bound and nonbound state in Hepes-based buffer. The assays were performed on a plate reader PHERAstar as described in the methods section. The error bars represent SEM (N = 3). GO, glucose oxidase; C, catalase; G, glucose

1.4. Oxygen Sensitivity of Luminescence of Free ARC-Lum(Fluo) Probes

The ARC-Lum(Fluo) probe ARC-1186 comprising the fluorescent dye Cy3B [Se(Cy3B)] was applied for the study of oxygen sensitivity of the luminescence of a free ARC-Lum(Fluo) probe. The GO-catalase method was applied for the generation of deoxygenated samples. Additional experiments were performed to show that the signal of free ARC-1186 is not caused by the after-glow of the excitation source or unspecific binding of the probe to nontarget proteins GO, catalase and BSA. The luminescence intensity of the labeled peptide Cy3B-r_9-NH_2 without the phosphorescent donor could not be distinguished from that of the buffer neither in enzymatically deoxygenated or nondeoxygenated conditions after a delay of 45 µs whether excited at at 330(60) nm or at 540(20) nm, whereas the TGL intensity of ARC-1186 if excited at 330(60) nm was proportional to the concentration within the concentration range from 3 to 100 nM (Figure 10). This means that the long-lifetime luminescence signal detected for free ARC-1186 was not caused by the after-glow of the xenon flash lamp. The addition of BSA or GO and catalase to the buffer solution did not change the luminescence lifetime of the probe.[92] The value of I_0 of free ARC-1186 [Se(Cy3B)] in deoxygenated conditions was 3.9 ± 0.5 times higher than that of the ARC-1138 [Se(-)], considering the transmittance of the emission filter, which passes 36% and 52% of the emission of ARC-1138 and ARC-1186, respectively, showing that the energy transfer from $^3D^*$ to A^1 also occurs in free ARC-1186.[92]

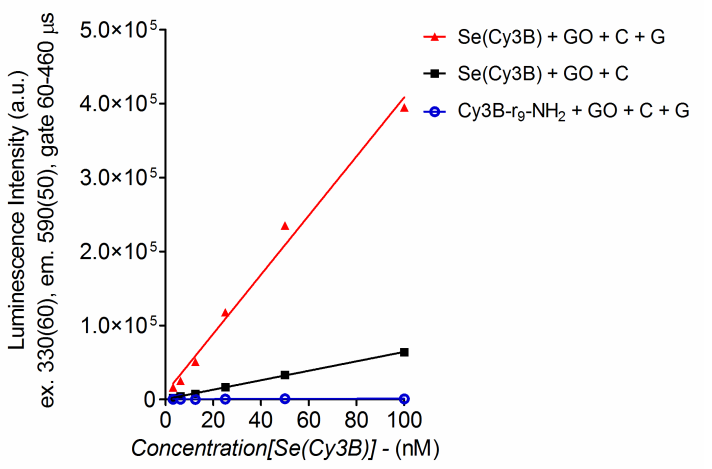

Figure 10. Oxygen sensitivity of TGL intensity of free ARC-1186 [Se(Cy3B)] ($R^2 > 0.98$). The concentration series of probe Se(Cy3B) and Cy3B-r_9-NH_2 was made in the presence of BSA (0.5 mg/mL). GO, glucose oxidase; C, catalase; G, glucose

1.5. Oxygen Sensitivity of Phosphorescence of Free ARC-Lum(-) Probes

The oxygen sensitivity of phosphorescence of ARC-Lum(-) probe ARC-1138 [Se(-)] was studied both in enzymatically deoxygenated conditions on a microplate as well as in argon-purged solution in a sealed cuvette. The luminescence of enzymatically deoxygenated samples was studied at 30 °C, whereas the argon-purged solutions were studied at room temperature. The phosphorescence lifetime of free ARC-1138 at room temperature in argon-purged buffer solution (τ = 290 ± 2 µs) was longer than the phosphorescence lifetime of ARC-1138 in complex with PKAc in nondeoxygenated buffer solution at room temperature (τ = 163 ± 7 µs). The longer luminescence lifetime of the deoxygenated sample with free ARC-1138 than that of the PK-bound probe ARC-1138 in the presence of molecular oxygen is in accordance with the increase of the luminescence lifetime of PK-bound ARC-1138 upon deoxygenation and shows that binding to the PK does not shield the luminophore from molecular oxygen completely. The luminescence lifetime of free ARC-1138 in Ar-purged solution at room temperature (τ = 290 ± 2 µs) was 2.5-fold longer than in enzymatically deoxygenated conditions at 30 °C (τ = 109.8 ± 3.4 µs). This difference in luminescence lifetimes of free Se(-) was not caused by temperature only (Figure 11). Although very small content of oxygen in enzymatically deoxygenated solution can still cause luminescence quenching of the free probe[27], additional quenching of phosphorescence by components of the enzymatic deoxygenation buffer may also be possible.[25]

1.6. Temperature Dependence of Microsecond-Scale Luminescence of ARC-Lum Probes

As studies with proteins are usually performed within the temperature range from room temperature to 37 °C, the effect of temperature on the microsecond-scale luminescence lifetime of ARC-Lum probes within this temperature range was studied in enzymatically deoxygenated conditions on a spectrofluorometer. The microsecond-scale luminescence lifetime of free ARC-1138 increased upon decrease of temperature and was linear within the temperature range from 20 °C to 37 °C (Figure 11). Also, slight increase of the luminescence lifetime of PK-bound ARC-1186 was observed at lower temperatures. For example, upon increase of temperature from 30 °C to 33 °C, the luminescence lifetime of PK-bound ARC-1186 decreased from 161 µs to 156 µs, i.e. by 4%, and that of free ARC-1138 from 135 µs to 128 µs, i.e. 5%. The results show that the temperature has to be tightly fixed and recorded within an assay with ARC-Lum probes if small changes of luminescence lifetime or integrated TGL intensity have to be detected.

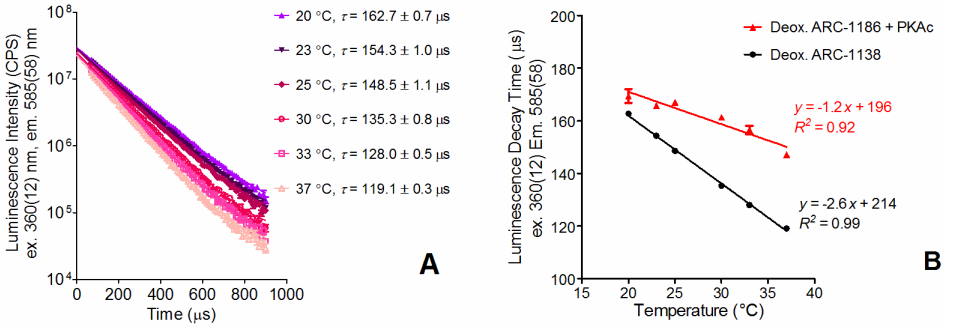

Figure 11. Temperature-dependence of free ARC-1138 and PK-bound ARC-1186 in enzymatically deoxygenated conditions in a sealed cuvette. Error bars represent SEM of two separate measurements within the same experiment.

1.7. Singlet-Singlet Energy Transfer in ARC-Lum(Fluo) Probes

Both fluorescence and phosphorescence spectrum of ARC-Lum(-) probes ARC-668 and ARC-1138 partly overlap with the absorption spectrum of fluorescent dyes Cy3B, TxR, and PF647. Therefore, in case of these fluorescent dyes, preconditions are fulfilled for realization of two types of energy transfer: firstly, for energy transfer from $^1D^*$ to ^1A ($^1D^* + {}^1A \rightarrow {}^1D + {}^1A^*$) and, secondly, for energy transfer from $^3D^*$ to ^1A ($^3D^* + {}^1A \rightarrow {}^1D + {}^1A^*$). The compounds comprising the fluorescent dye Cy3B, ARC-1186 and Cy3B-r_9-NH_2, were chosen for the study of FRET from $^1D^*$ to ^1A.

The efficiency of energy transfer from $^1D^*$ to ^1A was evaluated by comparison of the normalized steady-state emission spectra of ARC-1186 [Se(Cy3B)] and Cy3B-r_9-NH_2 (Figure 12 and equation 12). The obtained efficiency of energy transfer from $^1D^*$ to ^1A was very high – approximately 80%. The strong interaction between luminophores in free ARC-1186 may be caused by stacking of aromatic moieties in an aqueous buffer solution.

Förster distances that were determined by equation 4 for Se(Cy3B), Se(PF647), Se(TMR) and Se(TxR) were 2.2 nm, 2.0 nm, 2.0 nm and 2.0 nm, respectively (Table 2). The results suggest singlet-singlet FRET with similar efficiency to that in ARC-1186 [Se(Cy3B)] for the selenophene-comprising ARC-Lum probes with PF647, TMR or TxR as the acceptor-fluorophore. Furthermore, the similar singlet-singlet FRET efficiency leads to similar ISC efficiency. Therefore, the difference of microsecond-scale luminescence intensity (I_0) of these ARC-Lum(Fluo) probes is mainly caused by the difference in triplet-singlet FRET efficiency and the QY of the acceptor-fluorophore.

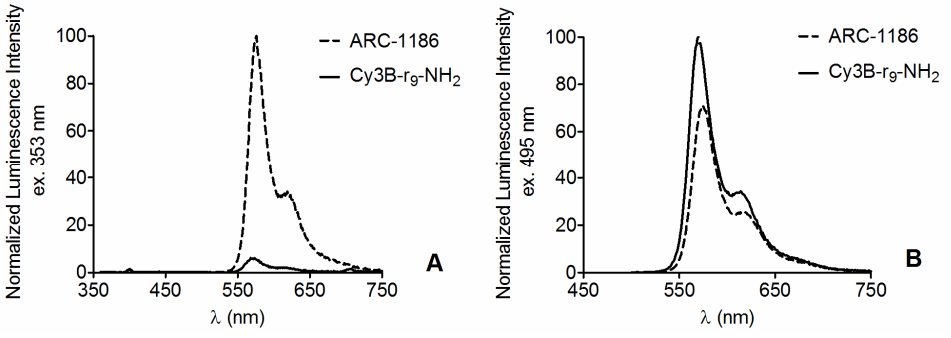

Figure 12. Comparison of luminescence emission spectrum of ARC-1186 [Se(Cy3B)] and Cy3B-r_9-NH_2. The steady-state emission spectra were recorded with excitation at 353 nm (A) and at 495 nm (B). The luminescence was calculated for 1 μM solution and then normalized by the shared maximal and minimal values.

Förster distances (equation 4) for singlet-singlet FRET were also determined for the thiophene-comprising ARC-Lum(Fluo) probes. Due to the 10-fold higher fluorescence QY of the probe ARC-668 [S(-)] than the fluorescence QY of ARC-1138 [Se(-)], the Förster distances for probes S(Cy3B), S(PF647), S(TMR) and S(TxR) were longer than those of their selenophene-containing counterparts: 3.1 nm, 2.4 nm, 2.5 nm and 2.5 nm, respectively (Table 2). These results suggest even higher singlet-singlet FRET efficiency for thiophene-containing ARC-Lum(Fluo) probes than for their selenophene-containing counterparts.

Table 2. Förster Distances and FRET Efficiencies of ARC-Lum(Fluo) Probes

Type of ARC-Lum(Fluo) probe	ARC-Lum(Fluo) probe	R_0 for $^1D^* \rightarrow {}^1A$ (nm)[a]	R_0 for $^3D^* \rightarrow {}^1A$ (nm)[b]	E for $^3D^* \rightarrow {}^1A$ (%)[c]
Se(Cy3B)	ARC-1186	2.2	2.6	29 ± 6
Se(PF647)	ARC-1139	2.0	3.1	69 ± 6
Se(TMR)	ARC-1144	2.0	2.2	45 ± 8
Se(TxR)	ARC-1185	2.0	2.7	51 ± 3
S(PF647)	ARC-1182	2.4	1.6	~19
S(TMR)	ARC-669	2.5	1.3	~16
S(TxR)	ARC-1134	2.5	1.4	~ 4
S(Cy3B)	-	3.1	1.6	ND

[a]The fluorescence emission spectra of free ARC-Lum(-) probes were applied in the calculations of Förster distance for FRET from $^1D^*$ to ^1A. [b]Förster distances calculated for FRET from $^3D^*$ to ^1A for thiophene-comprising compounds are based on the unpublished phosphorescence emission spectrum of the luminophore in ARC-668. [c]E has been calculated by equation 10 for the complex of the ARC-Lum(Fluo) probe and PKAc at 30 °C in nondeoxygenated buffer solution. One measurement has been performed with ARC-669 and ARC-1134. SEM has been shown for *E.* ND, not determined

The measurement of QYs showed decrease of luminescence intensity upon binding to PK in case of UV-excitation: the QY decreased from 56% to 29% (Paper III). This result shows that the interaction of luminophores is interfered upon binding. On the other hand, the decrease of singlet-singlet FRET efficiency in ARC-Lum(Fluo) probes upon binding to a PK may be also caused by the blue-shift of the fluorescence emission spectrum of the donor-luminophore, which leads to a smaller Förster distance for FRET from $^1D^*$ to ^1A (Figure 7 and equation 4). The decrease of singlet-singlet energy transfer efficiency enables more efficient ISC from $^1D^*$ to $^3D^*$; hence, it contributes to the increased microsecond-scale luminescence intensity of ARC-Lum(Fluo) probes upon binding to PKs. Therefore, minimization of the spectral overlap integral for singlet-singlet energy transfer together with the maximization of the spectral overlap integral for triplet-singlet energy transfer could be the principle applied in the design of ARC-Lum(Fluo) probes with high microsecond-scale luminescence intensity.

1.8. Triplet-Singlet Energy Transfer in Selenophene-Comprising ARC-Lum(Fluo) Probes

The efficiency of energy transfer from $^3D^*$ to ^1A was determined on the basis of luminescence lifetimes of the probes (equation 10). The calculated FRET efficiencies from $^3D^*$ to ^1A for ARC-1186 [Se(Cy3B)] in complex with PKAc were

29 ± 6 % and 65 ± 3% in nondeoxygenated and enzymatically deoxygenated solution, respectively (Paper III). These results are in accordance with the theory and show that if other modes of triplet deactivation are less competitive, the efficiency of the energy transfer from $^3D^*$ to ^1A increases as the luminescence lifetime of $^3D^*$ increases.[34]

Taking into account the FRET efficiency for triplet-singlet energy transfer in PK-bound ARC-1186 as determined by equation 10, the molar extinction coefficients of the donor and that of the acceptor at 350 nm, the phosphorescence QY of the donor (0.5%) and the QY of the acceptor (50%), it was possible to calculate the QY of donor-sensitized emission (including both singlet-singlet and triplet-singlet energy transfer) for PK-bound ARC-1186 in nondeoxygenated conditions, which was 26%. Based on this value it was estimated that the maximal efficiency of ISC and the corresponding QY of microsecond-scale luminescence of PK-bound ARC-1186 are 68% and 10%, respectively(SI of Paper III).

For comparison, we also characterized the luminescence of PK-bound ARC-1139 [Se(PF647)] in enzymatically deoxygenated conditions. ARC-1139 is a selenophene-comprising ARC-Lum(Fluo) probe conjugated with the fluorescent dye PF647 instead of the dye Cy3B (probe ARC-1186). The absorption spectrum of PF647 well overlaps with the phosphorescence emission spectrum of $^3D^*$ in Se(-). Also, the molar extinction coefficient at the absorption maximum of PF647 (ε = 250000 $M^{-1}cm^{-}1$) is almost two-fold higher than that of Cy3B at its absorption maximum (ε = 130000 $M^{-1}cm^{-1}$). As a result, the energy transfer from $^3D^*$ to ^1A is more efficient for PK-bound ARC-1139 (69 ± 6% in the presence of dissolved molecular oxygen) than for PK-bound ARC-1186. Due to the efficient FRET, rather fast depopulation of the $^3D^*$ takes place in the presence of PF647 and deoxygenation of the solution has smaller impact on the luminescence lifetime of ARC-1139 in complex with PKAc: the luminescence lifetime of PK-bound ARC-1139 increased only by 14 μs upon deoxygenation, from 33 μs to 47 μs (Figure 9 and Table 1). The calculated FRET efficiency for PK-bound ARC-1139 in deoxygenated solution was 89.5 ± 4.4%. This result shows that PF647 is a very good acceptor dye for $^3D^*$ in ARC-1139.

The calculated Förster distances and FRET efficiencies (Table 2) suggest higher proportion of triplet-singlet energy transfer and higher efficiency of ISC for PK-bound ARC-1139 if compared to PK-bound ARC-1186. It was estimated that if efficiency of ISC is 80%, the QY of microsecond-scale luminescence of PK-bound ARC-1139, which includes fluorophore PF647 (Φ ~ 30%), is $\Phi_{T\rightarrow S}$(ARC-1139) = 0.8×0.7×0.3 = 0.17, i.e., 17% in nondeoxygenated conditions and as $\Phi_{T\rightarrow S}$[Se(PF647)] = 0.8×0.9×0.3 = 0.22, i.e., 22% in enzymatically deoxygenated conditions. In comparison, the QYs of the Eu-based probes for biological assays ranged between 24–31% in water at 22 °C.[94] However, after a 50 μs long delay, almost 80% of the microsecond-scale luminescence of PK-bound ARC-1139 [Se(PF647)] has decayed in nondeoxygenated conditions. Hence, instruments that enable shorter delay time than those with a flash lamp would be more appropriate for assays with probe ARC-1139. On the other hand,

we looked for ways to increase the luminescence lifetime of the selenophene-comprising $^3D^*$ in PK-bound state. The structure that is conjugated to the luminophore in ARC-1138 was changed: one linker instead of two linkers and Ala-residue instead of Arg-residue were applied. The new probe ARC-1147 bound to PKAc with similar affinity compared to ARC-1138 (K_D < 0.2 nM), but the luminescence lifetime of PK-bound ARC-1147 was longer than that of PK-bound ARC-1138. Furthermore, the luminescence lifetime of the corresponding ARC-Lum(Fluo) probes in PK-bound state were longer than the conjugates of ARC-1138 and an acceptor-fluorophore: the luminescence lifetimes of PK-bound ARC-Lum(Fluo) probes ARC-1170 [Se(PF647)] and ARC-1148 [Se(TMR)] were τ = 46 ± 1 µs and τ = 92 ± 5 µs (N = 3), respectively, whereas the luminescence lifetimes of PK-bound ARC-1139 [Se(PF647)] and ARC-1144 [Se(TMR)] were τ = 36 ± 3 µs and τ = 59 ± 3 µs, respectively. The longer luminescence lifetime of PK-bound ARC-1170 than that of ARC-1139, lead to better SNR in case of gate 50–200 µs (Figure 13).

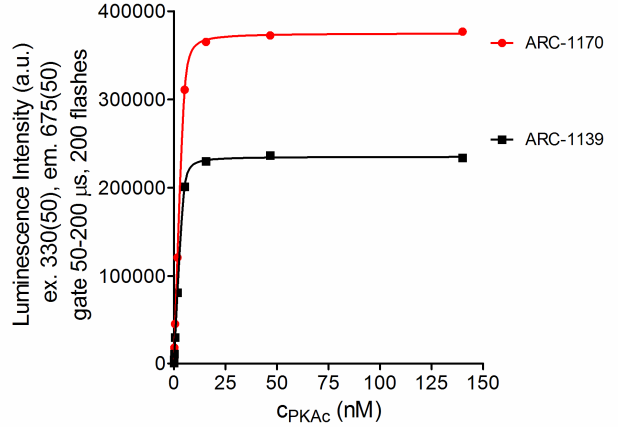

Figure 13. Titration of ARC-Lum(Fluo) probes ARC-1139 and ARC-1170 with PKAc.

1.9. Triplet-Singlet Energy Transfer in Thiophene-Comprising ARC-Lum(Fluo) Probes

Based on the comparison of the luminescence of PK-bound ARC-Lum(-) probes ARC-668 [S(-)] and ARC-1138 [Se(-)] (SI of Paper III) it was estimated that the phosphorescence QY of ARC-668 is 20-fold lower than that of Se(-), i.e., ~0.025%. Also, the phosphorescence emission spectrum of the luminophore in ARC-668 was blue-shifted if compared to that of the selenophene-comprising luminophore. Therefore, the Förster distances calculated for FRET from $^3D^*$ to ^1A for thiophene-comprising ARC-Lum(Fluo) probes were all shorter than those of selenophene-comprising ARC-Lum(Fluo) probes (Table 2). Despite the short Förster distance that was determined for thiophene-comprising

ARC-Lum(Fluo) probes, the probes were successfully applied in binding and displacement assays.[9,11] Furthermore, the luminescence intensity of the thiophene-comprising ARC-Lum(Fluo) probe ARC-1063 [S(AF647)] exceeded that of an Eu-cryptate in a practical application with biological samples.[95] Furthermore, the limit of detection was 4 pM (20 µL volume) for samples with PKAc.[95] Also, after a long delay, the luminescence of thiophene-comprising ARC-Lum(Fluo) probes is well comparable to their selenophene-comprising counterparts: after a ~140 µs long delay the remaining luminescence intensity of the thiophene-comprising probe ARC-1182 [S(PF647)] in PK-bound state exceeded that of the selenophene-comprising probe ARC-1139 [Se(PF647)] in PK-bound state and at a 200 µs long delay the luminescence intensity of PK-bound probe ARC-1182 equaled to that of its selenophene-comprising counterpart ARC-1139 in PK-bound state in nondeoxygenated conditions (the calculation is based on Table 1). The luminescence lifetime of PK-bound ARC-1182 showed more than 5-fold increase after enzymatic deoxygenation, from 109 to 556 µs (Table 1), which shows that FRET efficiency from $^3D^*$ to ^1A in PK-bound ARC-1182 in nondeoxygenated conditions cannot exceed 20%. The FRET efficiency that was determined for PK-bound ARC-1182 by equation 10 was 19 ± 5% (Table 2), which shows that upon deoxygenation, the FRET efficiency may exceed 90% as in case of selenophene-comprising ARC-1139.

Due to the short Förster distances for FRET from $^3D^*$ to ^1A in thiophene-comprising ARC-Lum(Fluo) probes, a modification was made to the structure of thiophene-comprising ARC-Lum(Fluo) probe: the acceptor-fluorophore was conjugated to the spacer (ARC-1085) and not to the peptidic moiety of the probe (ARC-1086). The more efficient triplet-singlet FRET in PK-bound ARC-1086 than in PK-bound ARC-1085 was confirmed by increased luminescence intensity and decreased microsecond-scale luminescence lifetime of the PK-bound probe (Figure 14).

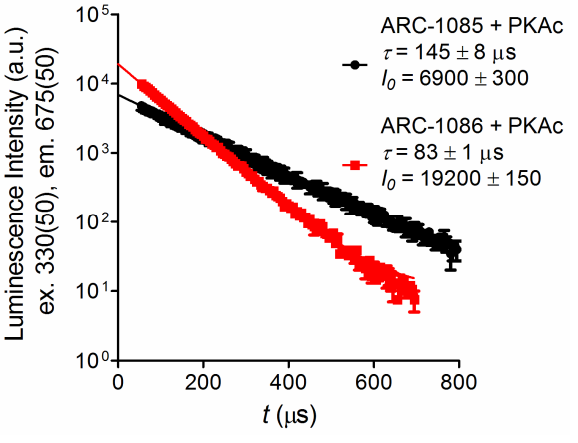

Figure 14. Luminescence decay of PK-bound ARC-Lum(Fluo) probes ARC-1085 and ARC-1086 (5 nM).

1.10. The Jablonski Diagram for ARC-Lum(Fluo) Probes

Based on the findings of the current study, a complemented Jablonski diagram was constructed for ARC-Lum(Fluo) probes (Figure 15). The current study showed that in addition to the FRET from the triplet state of the low-QY donor-luminophore to the singlet state of the high-QY acceptor-fluorophore ARC-Lum(Fluo) probes possess singlet-singlet energy transfer from the donor-luminophore to the acceptor-fluorophore. These two types of energy transfer (triplet-singlet and singlet-singlet) occur on a different time scale and in this study it was discovered that their proportion and efficiency depends on the environment surrounding the luminophores. If the probe is not bound to a PK, singlet-singlet energy transfer is efficient and $^3D^*$ is rapidly quenched by dissolved molecular oxygen and buffer components. Upon binding to a PK the energy transfer from $^1D^*$ to ^1A decreases and the probability of ISC increases. Furthermore, inside the active site of a PK $^3D^*$ is hindered from quenchers, which leads to longer lifetime of $^3D^*$ and enhanced efficiency of FRET from $^3D^*$ to ^1A. However, inside the catalytic pocket of the PK, the donor-luminophore is not fully shielded from the environment surrounding the PK and small quenchers, e.g., molecular oxygen, may still collide with the donor-luminophore during the lifetime of the excited triplet state. Therefore, the luminescence of the ARC-Lum/PK complex can be further increased by deoxygenation of the buffer solution.

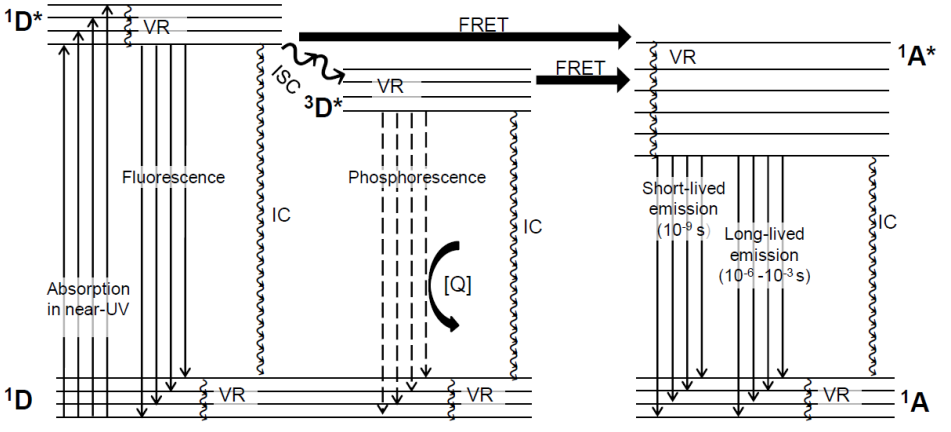

Figure 15. The Jablonski diagram of an ARC-Lum(Fluo) probe. The donor-luminophore (^1D) is excited with near-UV radiation. The excited donor-luminophore ($^1D^*$) can dissipate its energy via radiative (vertical solid lines) and nonradiative processes (curved lines), such as internal conversion (IC) and vibrational relaxation (VR). The presence of the acceptor-fluorophore (^1A) in close proximity to $^1D^*$ enables dipole-dipole interaction between the luminophores, leading to the relaxation of the donor-luminophore to the ground singlet state (^1D) and the formation of excited singlet state of the acceptor-luminophore ($^1A^*$) that thereafter emits photons and relaxes to the ground singlet state (^1A). $^1D^*$ can also change its spin by intersystem crossing (ISC) and go into excited triplet state $^3D^*$. In the presence of quenchers (Q), such as dissolved molecular oxygen, the energy of $^3D^*$ is dissipated mainly

by nonradiative processes and no phosphorescence occurs (the dashed vertical lines). If the concentration of the quencher is greatly reduced, e.g., inside the catalytic pocket of a PK, the lifetime of $^3D^*$ is increased. The increased lifetime of $^3D^*$ enables triplet-singlet energy transfer from $^3D^*$ to the conjugated acceptor-luminophore that leads to the relaxation of the donor to the ground singlet state ^1D and formation of $^1A^*$ that thereafter emits.

2. Application of ARC-Lum(Fluo) Probes in Live Cells (Paper I and Unpublished Data)

2.1. Characterization of ARC-Lum(Fluo) Probes

Two ARC-Lum probes, ARC-1185 [Se(TxR)] and ARC1188 [Se(TxR)], with different affinity towards PKAc (Figure 16) were chosen for the study of the activation of PKAc in live cells. ARC-Lum(Fluo) probes ARC-1185 and ARC-1188 comprise Ala-residue in the position of a chiral spacer in the structure of ARC-Lum probes (Figure 6). It has been shown that the Ala-residue in the position of a chiral spacer of an ARC-type inhibitor decreases the affinity of the probe towards the Rho-associated coiled-coil domain containing protein kinase II (ROCK-II) and the γ-isoform of protein kinase B (PKBγ), thereby increasing the selectivity of the probe towards PKAc.[93,96] Chirality of the spacer is also important and affects the affinity of the probe: ARC-1185, which comprises D-Ala, has much better affinity towards AGC PKs compared to ARC-1188, which comprises L-Ala (Table 3).

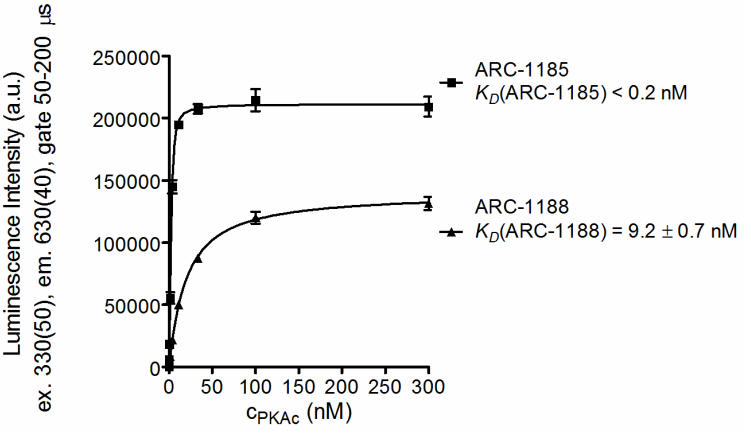

Figure 16. Titration of ARC-Lum(Fluo) probes ARC-1185 and ARC-1188 with PKAc. The error bars on the graph show standard deviation (SD) and the K_D value of ARC-1188 has been shown with 95% confidence intervals.

Table 3. Rough Estimations of the K_D Values of Complexes Comprising ARC-1185 or ARC-1188 and a PK*

Dissociation Constants of Complexes of ARC-1185 and ARC-1188 with PKs		
Protein kinase	***K_D of ARC-Lum(Fluo) probes* (nM)**	
	ARC-1185	***ARC-1188***
PKAc	< 0.2	9.2 ± 0.7
ROCK-II	< 0.2	0.8 ± 0.4
PKBγ (Akt3)	40 ± 20	160 ± 80
PKCδ	32 ± 20	245 ± 125
MSK-1	5 ± 4	185 ± 30
PIM-1	21 ± 8	20 ± 11

* 95% confidence intervals have been shown for K_D values. The correlation coefficient R^2 of the binding curves exceeded 0.95.

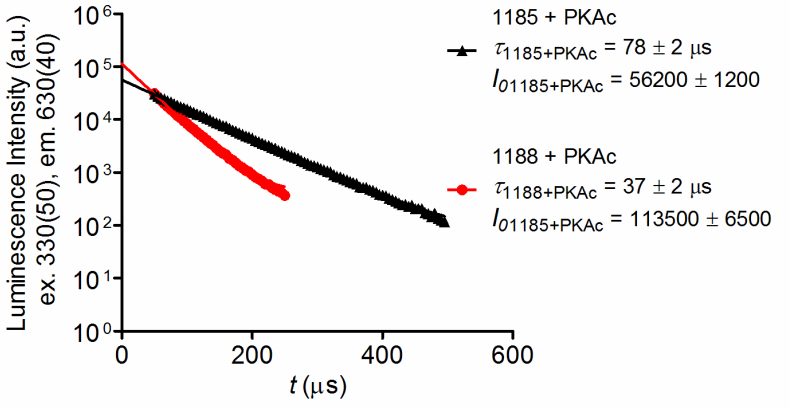

Figure 17. The luminescence decay of PK-bound ARC-Lum probes ARC-1185 and ARC-1188. The 95% confidence intervals have been shown for luminescence decay times (τ) and luminescence intensity extrapolated to t = 0 μs (I_0).

Although the K_D of the probe ARC-1185/PKAc complex is lower than the K_D of ARC-1188/PKAc complex, the values of luminescence brightness (I_0*τ) of the complexes do not differ: the luminescence decay time of ARC-1185 in complex with PKAc (τ = 78 ± 2 μs) is twice as long as that of ARC-1188 in complex with PKAc (τ = 37 ± 2 μs), but the extrapolated value of I_0 is two-fold lower (Figure 17). Hence, the luminescence intensities of ARC-1185 and ARC-1188 if bound to PKAc at 50 μs long delay are almost the same. However, 47% and 74% of the microsecond-scale luminescence of ARC-1185 and ARC-1188 in

complex with PKAc has decayed after 50 μs long delay, respectively. Therefore, ARC-1185 is more suitable for assays performed on a plate reader with a xenon flash lamp as the excitation source. An LED was used as an excitation source for TGL microscopy and a delay as short as 10 μs could be applied. After a delay of 10 μs only 13% and 24% of the luminescence emission of ARC-1185/PKAc and ARC-1188/PKAc complexes has decayed, respectively.

2.2. TGL Microscopy

The reliability of the instrumentation applied for TGL microscopy with the delay of 10 μs was controlled by the application of the compound TxR-r_9-NH_2. TxR-r_9-NH_2 is the cell penetrating peptide (CPP) nona(D-arginine)amide labeled with the fluorescent dye TxR. Although there was a strong fluorescence signal, no TGL signal originating from TxR-r_9-NH_2 could be detected after a delay of 10 μs (Figure 18).

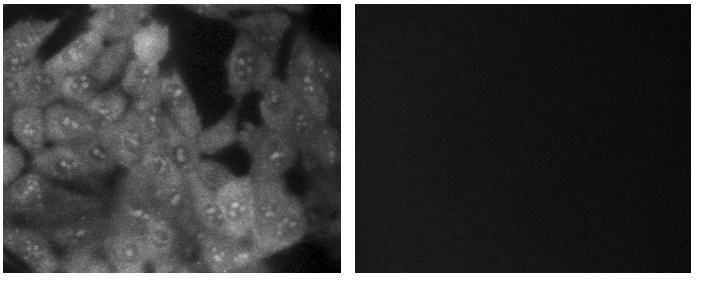

Figure 18. Localization profile of TxR-r_9-NH2 in MDCKII cells imaged with the fluorescence microscope (left) and the TGL microscope (right).

A TGL image could be obtained with the probe ARC-1185 using the same settings (Figure 19). Fluorescence and TGL images representing the localization profile of ARC-1185 in cells and the localization profile of the complex(es) of ARC-1185 with basophilic PKs generally overlapped (Figure 19). This can be explained with the high affinity of ARC-1185 towards several basophilic PKs as a result of which the localization profile of the luminescent probe reflects the activity of basophilic PKs in cells. Furthermore, the similarity of the localization profile of TxR-r_9-NH_2 and ARC-1185 in MDCKII cells may be the result of binding of the positively charged peptide TxR-r_9-NH_2 to basophilic enzymes PKAc and PKC[97], furins[98] and/or DNA[99].

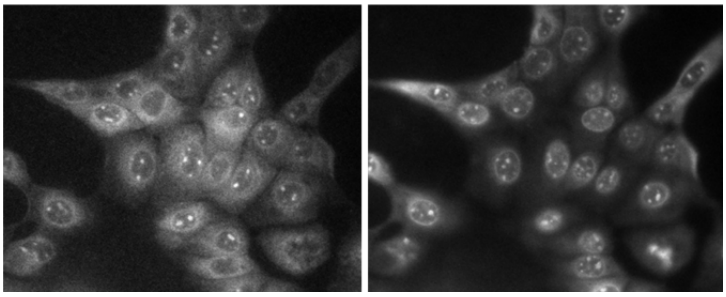

Figure 19. Localization profile of ARC-1185 in MDCKII cells imaged with the fluorescence microscope (left) and the TGL microscope (right).

Next, probes ARC-1185 and ARC-1188 were applied to monitor and map the activity of PKAc in live cells. The probe ARC-1185 or ARC-1188 was added to the cells together with or without the activators of PKA (FRSK and IBMX). TGL images were taken during the period of 2 hours. The experiments were repeated for three times both with and without the addition of FRSK and IBMX. The results of the time-lapse assays are shown in Figures 20–21. The images could be successfully recorded without any interfering signal from the incubation solution containing the ARC-Lum(Fluo) probe on the cells. The persistent difference between cells with unactivated and activated PKAc was the rapid formation of the TGL signal in cells incubated with FRSK and IBMX (Figure 20). Similar images were obtained with probes ARC-1185 and ARC-1188: both ARC-Lum(Fluo) probes rapidly entered the cells and responded to the dissociation of PKAc from the PKA holoenzyme upon activation with FRSK and IBMX. However, probe ARC-1185 provided a slightly better SNR.

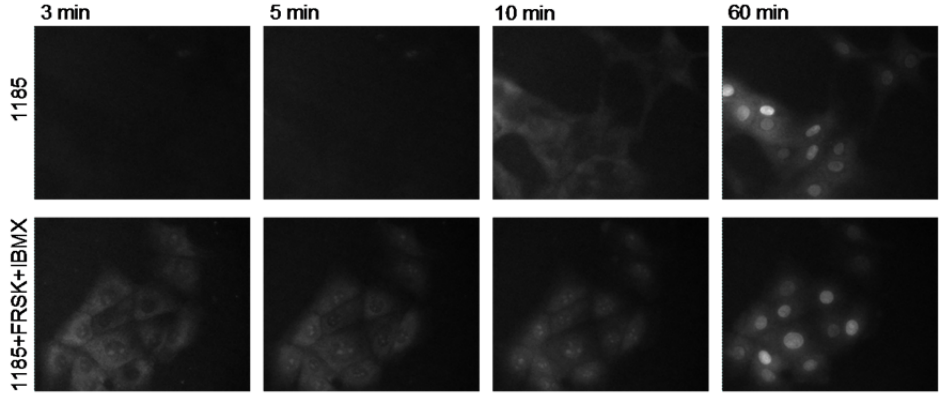

Figure 20. Formation of the ARC-1185/kinase complex in MDCKII cells treated or not treated with FRSK and IBMX as monitored with the TGL microscope.

The relocation of probes ARC-1185 and ARC-1188 into the nucleus 10-20 min after the addition of FRSK and IBMX is an expected result: activated PKAc can freely diffuse into the nucleus, where it catalyses the phosphorylation of several transcription factors, e.g., CREB. However, this relocation also occurred after a slightly longer incubation time (30-45 min) if cells were incubated with the probe ARC-1185 or ARC-1188 only (Figures 20 and 21). Furthermore, the localization profile of the TGL signal in activated and unactivated cells was the same after 60 min of the addition of the luminescent probe ARC-1185 (Figure 20) or ARC-1188. This indicates that probes ARC-1185 and ARC-1188 may bind to other basophilic kinases which activity does not directly depend on the concentration of cAMP inside the cells, *e.g.,* MSK-1 that is active in the nucleus[100]. Also, unspecific binding to other biomolecules in the cell nucleus is possible. Another reason could be that as the concentration of the probe inside cells increases, the equilibrium between the PKA holoenzyme and PKAc is altered and more free PKAc is formed, which can then diffuse into nucleus with the ARC-Lum(Fluo) probe.

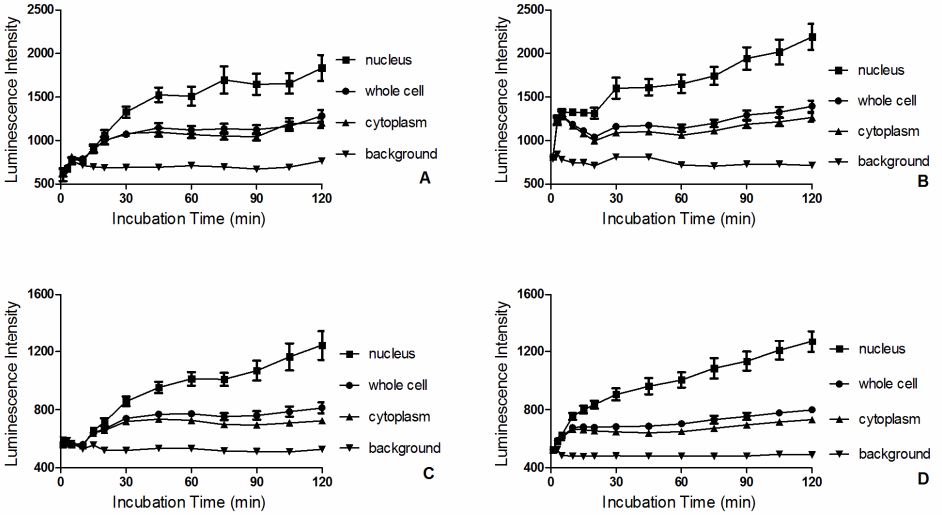

Figure 21. Comparison of the intensity of the TGL signal of ARC- 1185/kinase (A and B) and ARC/1188 complexes (C and D) in MDCKII cells treated (B and D) or not treated with FRSK and IBMX (A and C). Each point on the graph represents TGL signal averaged over 3x9 cells imaged on three different days. The error bars represent SEM.

A biochemical assay was performed to assure that the intense luminescence signal of ARC-1185 in cell nucleus is not caused by binding to DNA (Paper I). The fluorescence anisotropy readout showed that the probe ARC-1185 bound to DNA with more than 500-fold lower affinity if compared to its affinity towards

PKAc (Paper I). Furthermore, no microsecond-scale luminescence could be detected upon binding to DNA (Paper I).

To conclude, the luminescence properties of ARC-Lum(Fluo) probes ARC-1185 and ARC-1188 are suitable for the study of PK activity in living cells by TGL microscopy, but further studies have to be accomplished to determine whether the affinity or the selectivity of the probes should be altered for reliable monitoring of the dynamics of PKAc. For this, different inhibitors and activators of PKs, e.g., PKAc inhibitor protein (PKI) or ROCK inhibitor Y-27632, could be applied together with ARC-Lum(Fluo) probes. Also, various incubation times and concentrations of ARC-Lum probes could be tested to alter the uptake and intracellular concentration of the probes. In addition, studies of cytotoxicity of the ARC-Lum probes should be performed.

SUMMARY

This work further discloses photoluminescent properties of unique PK binding-responsive organic probes, ARC-Lum(Fluo) probes, that possess luminescence decay time in the microsecond range. An ARC-Lum(Fluo) probe is a tandem-luminophore that incorporates a low-QY donor-phosphor linked to a long-wavelength short-lifetime acceptor with high QY. The long-lifetime donor induces slow decay from the acceptor, which is due to FRET from the excited triplet state of the donor ($^3D^*$) to the singlet state of the acceptor. The energy is stored in $^3D^*$ and released gradually via FRET to the acceptor-fluorescent dye, leading to $^1A^*$ of the latter and the following light emission from the dye.

Firstly, the phosphorescence emission spectrum of the donor-luminophore was very broad and therefore various dyes could be applied as acceptor-fluorophores in ARC-Lum(Fluo) probes, leading to probes with different FRET efficiency and microsecond-scale luminescence lifetimes. The current study showed that the TGL excitation spectra of these PK-bound ARC-Lum(Fluo) probes coincided with that of the donor-luminophore. The fluorescent dye PF647 was the most suitable acceptor dye for $^3D^*$ in ARC-1138 [Se(-)] with the FRET efficiency close to 90% in enzymatically deoxygenated conditions. The estimated QY of microsecond-scale luminescence of PK-bound ARC-1139 [Se(PF647)] in nondeoxygenated conditions was ~17%. However, the efficient FRET led to rather short luminescence lifetime of PK-bound probe ARC-1139 (τ = 36 μs) and therefore the thiophene-comprising counterpart of ARC-1139, probe ARC-1182, which had 3-fold longer lifetime in PK-bound state in nondeoxygenated conditions if compared to probe ARC-1139, would be more suitable for practical applications that require delay times longer than 140 μs.

Secondly, it was discovered that in addition to FRET from $^3D^*$ to ^1A ARC-Lum(Fluo) probes possess singlet-singlet energy transfer from $^1D^*$ to ^1A. These two types of energy transfer (triplet-singlet and singlet-singlet, respectively) occur on a different time scale and their efficiency and proportion depend on the environment surrounding the luminophores. If the probe is not bound to a PK, singlet-singlet energy transfer is efficient and $^3D^*$ is rapidly quenched by dissolved molecular oxygen and buffer components. Upon binding to a PK energy transfer from $^1D^*$ to ^1A decreases and the efficiency of ISC increases. Furthermore, inside the active site of a PK $^3D^*$ is hindered from quenchers, such as dissolved molecular oxygen, leading to longer lifetime of $^3D^*$ and enhanced efficiency of FRET from $^3D^*$ to ^1A. Minimization of the spectral overlap integral for singlet-singlet energy transfer together with the maximization of the spectral overlap integral for triplet-singlet energy transfer could be the principle applied in the design of ARC-Lum(Fluo) probes with high microsecond-scale luminescence intensity.

Thirdly, the microsecond-scale luminescence decay time and thereby the luminescence of the ARC-Lum/PK complex can be further increased by deoxygenation of the buffer solution. Luminescence lifetimes as long as half a millisecond were determined for thiophene-comprising ARC-Lum(Fluo) probes in

complex with a PK in enzymatically deoxygenated conditions on unsealed microplates, making the probes well suitable for high-throughput studies with the application of a commonly used xenon flash lamp as the excitation source. Also, the strong oxygen-sensitivity of the luminescence of ARC-Lum probes enables them to be applied as probes for molecular oxygen in the future.

Fourthly, the ARC-Lum(Fluo) probes were applied for mapping and monitoring of the activity of PKs in live cells with TGL microscopy. The probes entered the cells within a few minutes and produced a microsecond-scale luminescence signal that could be effectively distinguished from the autofluorescence of cells and the fluorescence of the acceptor dye. Furthermore, the probes responded to the activation of PKAc by rapid formation of the TGL signal.

To conclude, this study points to a settlement that helps to surpass the low QY of organic phosphors in aqueous solution at room temperature. An efficient FRET from $^{3}D^{*}$ to ^{1}A leads to substantially increased QY (here more than 75-fold increase was obtained) of the donor-acceptor pair, resulting in bright tandem probes possessing microsecond-scale emission lifetime, large pseudo-Stokes shift, and emission in orange or red spectral region. Probes with microsecond-scale luminescence lifetime can be applied with TR luminescence measurement techniques, which effectively reduce the strong autofluorescence of biological samples that have mainly nanosecond-scale lifetime, leading to increased sensitivity of the assay.

SUMMARY IN ESTONIAN

Mikrosekundilise luminestsentsi elueaga orgaaniliste sondide iseloomustamine ja rakendamine proteiinkinaaside uurimiseks

Ensüümid osalevad signaaliülekande- ja ainevahetusradades, mõjutades seeläbi rakkude arengut ja kasvu ning rakkude reaktsioone keskkonnatingimustele. Ensüümide tavapärasest erinev kolmedimensionaalne struktuur, lokalisatsioon ja aktiivsus rakkudes võib põhjustada organismi haiguslikke seisundeid. Selleks, et kõrvalekaldeid ensüümide tavapärastest omadustest detekteerida juba muutuste varajases arengujärgus, on vaja arendada tundlikke mõõtmismeetodeid. Käesolevas töös uuriti süvitsi ühte võimalikku lähenemist tundlike meetodite arendamisele ensüümide detekteerimiseks orgaaniliste ühendite abil bioloogilistes proovides.

Uurimistöös kasutati Tartu Ülikooli keemia instituudis välja arendatud fotoluminestsentssonde [ARC-Lum(Fluo) sonde], mille luminestsentsomadused muutuvad oluliselt seondumisel aktiivsetele proteiinkinaasidele: ensüümidele, mis katalüüsivad elusrakkudes nukleosiidtrifosfaadi γ-fosforüülrühma ülekannet seriini, treoniini või türosiini jääkidele valkudes. Kui proteiinkinaasidele seondunud ARC-Lum(Fluo) sonde ergastada ultravioletse kiirgusega, siis emiteerivad need pikaealist fotoluminestsentskiirgust, mille eluiga jääb mikrosekundilisse suurusjärku. ARC-Lum(Fluo) sondide pikk luminestsentsi eluiga kompleksis proteiinkinaasiga võimaldab kasutada kompleksi detekteerimiseks aegviivitusega mõõtmistehnikaid, mis tagavad pikaealise luminestsentsi selge eristamise bioloogiliste proovide autofluorestsentsist, mille eluiga jääb tavapäraselt nanosekundilisse suurusjärku. Ühtlasi on tagatud mõõtmismeetodi hea signaal-müra suhe ning võimaldatud proteiinkinaaside detektsioon väga väikeses kontsentratsioonis.

ARC-Lum(Fluo) sondide eredus kompleksis proteiinkinaasiga on tagatud molekulisisese Försteri resonantse energiaülekandega (edaspidi energiaülekanne) madala kvantsaagisega doonor-luminofoorilt (edaspidi doonor) kõrge kvantsaagisega aktseptor-fluorofoorile (edaspidi aktseptor): ergastusel neelatud valgusenergiat säilitatakse doonori ergastatud tripletsel olekul, kust see kantakse üle singletses olekus aktseptorile, mille tulemusel aktseptor ergastub ja kiirgab neelatud energia fluorestsentsina ning taastatakse doonori ja aktseptori singletne põhiolek. Selle energiaülekande tulemusel läheneb sondi kvantsaagise väärtus aktseptori kvantsaagise väärtusele, kuid aktseptorilt kiirguva luminestsentsi eluiga on doonor-vahendatud ergastuse korral oluliselt pikem kui aktseptori otseergastuse korral. Käesolevas uurimistöös iseloomustati ARC-Lum(Fluo) sondides toimuvaid energiaülekandeid mõjutavaid keemilis-füüsikalisi tegureid nii sondi vabas kui proteiinkinaasiga seondunud olekus; kvantifitseeriti ARC-Lum(Fluo) sondide pikaealise luminestsentsi eredus ja rakendati ARC-Lum(Fluo) sonde proteiinkinaaside jälgimiseks ja kaardistamiseks elusates rakkudes aegviivitusega mikroskoopia abil.

Esiteks leidis uurimistöös kinnitust, et ARC-Lum(Fluo) sondide aegviivitusega luminestsentsi ergatusspekter on määratud doonoriga ning selle kuju on sõltumatu aktseptorist. Doonori fosforestsentsi kiirgusspektri suur ulatus võimaldas mitmete erinevate fluorestsentsvärvide kasutamist aktseptorina ARC-Lum(Fluo) sondides. Ühtlasi, oli aktseptori valikuga võimalik mõjutada energiaülekande efektiivsust ja ARC-Lum(Fluo) sondi mikrosekundilise luminestsentsi eluiga. Kõike suurem energiaülekande efektiivsus selenofeeni sisaldava doonori ergastatud tripletse oleku ja aktseptori singletse oleku vahel (E = 89%) saavutati fluorestsentsvärvi PromoFluor647 kasutamisel aktseptorina. Vastava ARC-Lum(Fluo) sondi kvantsaagis (Φ ~ 17%) oli võrreldav mõnede lantaniidi-põhiste metalli-ligandi komplekside kvantsaagistega sarnastes tingimustes (Φ = 24 – 31%). Samas leiti, et mõõtmistes, kus ergastusele järgneva viivituse pikkus ületab 140 μs, on otstarbekam kasutada sama sondi tiofeeni sisaldavat analoogi, sest selle luminestsentsi eluiga on oluliselt (lahustunud hapniku juuresolekul 3 korda) pikem.

Teiseks avastati uurimistöö käigus, et lisaks Försteri resonantsele energiaülekandele doonori ergastatud tripletselt olekult aktseptori singletsele olekule toimub ARC-Lum(Fluo) sondides energiaülekanne doonori ergastatud singletselt olekult aktseptori singletsele olekule. Need kaks energiaülekannet (tripletilt-singletile ja singletilt-singletile) toimuvad erineval ajaskaalal ning nende osakaal ja efektiivsus sõltuvad sondi ümbritsevast keskkonnast. Kui ARC-Lum(Fluo) sond on vabalt lahuses, siis on energiaülekanne singletilt-singletile väga efektiivne ning doonori tripletne olek on kustutatud vesilahuses lahustunud molekulaarse hapniku poolt. Seondumisel proteiinkinaasile väheneb singletilt-singletile toimuva energiaülekande efektiivsus ja suureneb süsteemidevahelise ülekande efektiivsus ehk moodustub rohkem doonori ergastatud tripletset olekut. Lisaks on doonori ergastatud tripletne olek proteiinkinaasile seondunult varjestatud puhvris sisalduvate komponentide, seal hulgas molekulaarse hapniku, eest, mistõttu doonori ergastatud tripletse oleku eluiga pikeneb. Ühtlasi suureneb doonori ergastatud tripletselt olekult aktseptorile toimuva energiaülekande efektiivsus. Siiski pole varjestusefekt täielik, mistõttu proteiinkinaasile seondund ARC-Lum(Fluo) sondi luminestsentsi eluiga pikeneb lahusest molekulaarse hapniku eemaldamisel veelgi, näiteks tiofeeni sisaldava doonoriga ARC-Lum(Fluo) sondi ARC-1182 luminestsentsi eluiga hapnikuvabas lahuses proteiinkinaasile seondunult oli pikem kui pool millisekundit. Nii pika luminestsentsi elueaga sondid sobivad kiirsõelumisuuringuteks, kus tavapäraseks ergastusallikaks on välklamp, mis järelhelenduse tõttu vajab pika viivituse rakendamist pärast ergastusimpulssi.

Kolmandaks rakendati ARC-Lum(Fluo) sonde edukalt proteiinkinaaside aktiivsuse seireks ja kaardistamiseks uudse meetodi, aegviivitusega mikroskoopia abil. Kasutatud ARC-Lum(Fluo) sondid läbisid raku plasmamembraani mõne minutiga ja rakkude kiiritamisel ultraviolettkiirgusega emiteerisid rakkudes mikrosekundilise elueaga luminestsentsi, mis oli selgelt eristatav rakkude autofluorestsentsist ja aktseptori fluorestsentsist.

Käesolevas uurimistöös kirjeldati üht lahendust tundlike mikrosekundilise elueaga orgaaniliste luminestsentssondide arendamiseks. Sellise lahenduse alusel arendatud sonde iseloomustab lisaks pikale luminestsentsi elueale suur pseudo-Stokesi nihe ja emissioon nähtava spektri punases alas. Taoliste sondide rakendamine katsetes bioloogiliste proovidega, kasutates luminestsenentsi detektsiooniks aegviivitusega mõõtmismeetodeid, tagab hea signaal-müra suhte ja suurendab mõõtmismeetodite tundlikkust.

REFERENCES

(1) Amoroso, A. J.; Pope, S. J. A. Using Lanthanide Ions in Molecular Bioimaging. *Chem. Soc. Rev.* **2015**, *44* (14), 4723–4742.

(2) Rajendran, M.; Miller, L. W. Evaluating the Performance of Time-Gated Live-Cell Microscopy with Lanthanide Probes. *Biophys. J.* **2015**, *109* (2), 240–248.

(3) Murphy, L.; Congreve, A.; Pålsson, L.-O.; Williams, J. a G. The Time Domain in Co-Stained Cell Imaging: Time-Resolved Emission Imaging Microscopy Using a Protonatable Luminescent Iridium Complex. *Chem. Commun. (Camb).* **2010**, *46*, 8743–8745.

(4) Thibon, A.; Pierre, V. C. Principles of Responsive Lanthanide-Based Luminescent Probes for Cellular Imaging. *Anal. Bioanal. Chem.* **2009**, *394* (1), 107–120.

(5) Mukherjee, S.; Thilagar, P. Recent Advances in Purely Organic Phosphorescent Materials. *Chem. Commun.* **2015**, *51* (55), 10988–11003.

(6) Allain, C.; Faulkner, S. Photophysical Approaches to Responsive Optical Probes. *Future Med. Chem.* **2010**, *2* (3), 339–350.

(7) Piszczek, G. Luminescent Metal-Ligand Complexes as Probes of Macromolecular Interactions and Biopolymer Dynamics. *Arch. Biochem. Biophys.* **2006**, *453* (1), 54–62.

(8) Papkovsky, D. B.; O'Riordan, T. C. Emerging Applications of Phosphorescent Metalloporphyrins. *J. Fluoresc.* **2005**, *15* (4), 569–584.

(9) Enkvist, E.; Vaasa, A.; Kasari, M.; Kriisa, M.; Ivan, T.; Ligi, K.; Raidaru, G.; Uri, A. Protein-Induced Long Lifetime Luminescence of Nonmetal Probes. *ACS Chem. Biol.* **2011**, *6* (10), 1052–1062.

(10) Ekambaram, R.; Enkvist, E.; Manoharan, G. B.; Ugandi, M.; Kasari, M.; Viht, K.; Knapp, S.; Issinger, O.-G.; Uri, A. Benzoselenadiazole-Based Responsive Long-Lifetime Photoluminescent Probes for Protein Kinases. *Chem. Commun. (Camb).* **2014**, *50*, 4096–4098.

(11) Kasari, M.; Ligi, K.; Williams, J. A. G.; Vaasa, A.; Enkvist, E.; Viht, K.; Pålsson, L. O.; Uri, A. Responsive Microsecond-Lifetime Photoluminescent Probes for Analysis of Protein Kinases and Their Inhibitors. *Biochim. Biophys. Acta - Proteins Proteomics* **2013**, *1834* (7), 1330–1335.

(12) Vaasa, A.; Ligi, K.; Mohandessi, S.; Enkvist, E.; Uri, A.; Miller, L. W. Time-Gated Luminescence Microscopy with Responsive Nonmetal Probes for Mapping Activity of Protein Kinases in Living Cells. *Chem. Commun.* **2012**, *48* (68), 8595–8597.

(13) Ekambaram, R.; Manoharan, G. babu; Enkvist, E.; Ligi, K.; Knapp, S.; Uri, A. PIM Kinase-Responsive Microsecond-Lifetime Photoluminescent Probes Based on Selenium-Containing Heteroaromatic Tricycle. *RSC Adv.* **2015**, *5* (117), 96750–96757.

(14) Stennett, E. M. S.; Ciuba, M. A.; Levitus, M. Photophysical Processes in Single Molecule Organic Fluorescent Probes. *Chem. Soc. Rev.* **2014**, *43* (4), 1057–1075.

(15) McNaught, A. D.; Wilkinson, A.; Nic, M.; Jirat, J.; Kosata, B.; Jenkins, A. IUPAC. Compendium of Chemical Terminology, 2nd ed. (The "Gold Book", version 2.3.3.) http://goldbook.iupac.org/index.html (accessed Apr 11, 2014).

(16) Lakowicz, J. R. Introduction to Fluorescence. In *Principles of Fluorescence Spectroscopy*; Springer US, 2006; bll 1–26.

(17) Lower, S. K.; El-Sayed, M. A. The Triplet State and Molecular Electronic Processes in Organic Molecules. *Chem. Rev.* **1966**, *66* (2), 199–241.

(18) Sauer, M.; Hofkens, J.; Enderlein, J. Basic Principles of Fluorescence Spectroscopy. In *Handbook of Fluorescence Spectroscopy and Imaging*; Wiley-VCH Verlag GmbH&Co. KGaA: Weinheim, 2011; bll 1–29.
(19) Albani, J. R. Fluorescence Quenching. In *Principles and Applications of Fluorescence Spectroscopy*; Blackwell Publishing, 2007; bll 139–159.
(20) Wang, X.; Wolfbeis, O. S.; Meier, R. J. Luminescent Probes and Sensors for Temperature. *Chem. Soc. Rev.* **2013**, *42* (19), 7834–7869.
(21) Lakowicz, J. R. Quenching of Fluorescence. In *Principles of Fluorescence Spectroscopy*; Springer US: Boston, MA, 2006; bll 278–330.
(22) Sapsford, K. E.; Berti, L.; Medintz, I. L. Materials for Fluorescence Resonance Energy Transfer Analysis: Beyond Traditional Donor-Acceptor Combinations. *Angew. Chem. Int. Ed. Engl.* **2006**, *45* (28), 4562–4589.
(23) Braslavsky, S. E.; Fron, E.; Rodríguez, H. B.; Román, E. S.; Scholes, G. D.; Schweitzer, G.; Valeur, B.; Wirz, J. Pitfalls and Limitations in the Practical Use of Förster's Theory of Resonance Energy Transfer. *Photochem. Photobiol. Sci.* **2008**, *7* (12), 1444–1448.
(24) Kowalska-Baron, A.; Gałęcki, K.; Wysocki, S. Photophysics of Indole-2-Carboxylic Acid (I2C) and Indole-5-Carboxylic acid (I5C): Heavy Atom Effect. *Spectrochim. Acta Part A Mol. Biomol. Spectrosc.* **2013**, *116*, 183–195.
(25) Banks, D. D.; Kerwin, B. A. A Deoxygenation System for Measuring Protein Phosphorescence. *Anal. Biochem.* **2004**, *324* (1), 106–114.
(26) Baumann, R. P.; Penketh, P. G.; Seow, H. A.; Shyam, K.; Sartorelli, A. C. Generation of Oxygen Deficiency in Cell Culture Using a Two-Enzyme System to Evaluate Agents Targeting Hypoxic Tumor Cells. *Radiat. Res.* **2008**, *170* (5), 651–660.
(27) Englander, S. W.; Calhoun, D. B.; Englander, J. J. Biochemistry without Oxygen. *Anal. Biochem.* **1987**, *161* (2), 300–306.
(28) Scholes, G. D. Long-Range Resonance Energy Transfer in Molecular Systems. *Annu. Rev. Phys. Chem.* **2003**, *54*, 57–87.
(29) Sauer, M.; Hofkens, J.; Enderlein, J. Excited State Energy Transfer; Wiley-VCH Verlag GmbH&Co. KGaA; bll 147–188.
(30) Shrestha, D.; Jenei, A.; Nagy, P.; Vereb, G.; Szöllősi, J. Understanding FRET as a Research Tool for Cellular Studies. *Int. J. Mol. Sci.* **2015**, *16* (4), 6718–6756.
(31) Yuan, L.; Lin, W.; Zheng, K.; Zhu, S. FRET-Based Small-Molecule Fluorescent Probes: Rational Design and Bioimaging Applications. *Acc. Chem. Res.* **2013**, *46* (7), 1462–1473.
(32) Förster, T. Zwischenmolekulare Energiewanderung und Fluoreszenz. *Ann. Phys.* **1948**, *437* (1-2), 55–75.
(33) Förster, T. 10th Spiers Memorial Lecture. Transfer Mechanisms of Electronic Excitation. *Discuss. Faraday Soc.* **1959**, *27*, 7–17.
(34) Rohatgi-Mukherjee, K. K. Fundamentals of Photochemistry; New Age International, 1978; bl 197.
(35) Lakowicz, J. R. Theory of Energy Transfer for a Donor-Acceptor Pair. In *Principles of Fluorescence Spectroscopy*; Lakowicz, J. R., Red; Springer US: Boston, MA, 2006; bll 445–451.
(36) *FRET - Förster Resonance Energy Transfer: From Theory to Applications*; Medintz, I., Hildebrandt, N., Reds; Wiley-VCH Verlag GmbH&Co. KGaA, 2014.

(37) Hildebrandt, N. How to Apply FRET: From Experimental Design to Data Analysis. In *FRET – Förster Resonance Energy Transfer: From Theory to Applications*; Medintz, I., Hildebrandt, N., Reds; Wiley-VCH Verlag GmbH&Co. KGaA, 2014; bll 105–163.
(38) Dos Remedios, C. G.; Moens, P. D. Fluorescence Resonance Energy Transfer Spectroscopy Is a Reliable "Ruler" for Measuring Structural Changes in Proteins. Dispelling the Problem of the Unknown Orientation Factor. *J. Struct. Biol.* **1995**, *115* (2), 175–185.
(39) Lakowicz, J. R. Energy Transfer. In *Principles of Fluorescence Spectroscopy*; Springer US, 2006.
(40) Stobiecka, M.; Chałupa, A. Biosensors Based on Molecular Beacons. *Chem. Pap.* **2015**, *69* (1), 62–76.
(41) Selvin, P. R. Principles and Biophysical Applications of Lanthanide-Based Probes. *Annu. Rev. Biophys. Biomol. Struct.* **2002**, *31*, 275–302.
(42) Hildebrandt, N.; Wegner, K. D.; Algar, W. R. Luminescent Terbium Complexes: Superior Förster Resonance Energy Transfer Donors for Flexible and Sensitive Multiplexed Biosensing. *Coord. Chem. Rev.* **2014**, *273-274*, 125–138.
(43) Vogel, K. W. Improving Lanthanide-Based Resonance Energy Transfer Detection by Increasing Donor-Acceptor Distances. *J. Biomol. Screen.* **2006**, *11* (4), 439–443.
(44) Vereb, G.; Jares-Erijman, E.; Selvin, P. R.; Jovin, T. M. Temporally and Spectrally Resolved Imaging Microscopy of Lanthanide Chelates. *Biophys. J.* **1998**, *74* (5), 2210–2222.
(45) Bünzli, J.-C. G. Lanthanide Light for Biology and Medical Diagnosis. *J. Lumin.* **2016**, *170*, 866–878.
(46) Connally, R. E.; Piper, J. A. Time-Gated Luminescence Microscopy. *Ann. N. Y. Acad. Sci.* **2008**, *1130* (1), 106–116.
(47) Lakowicz, J. R. Fluorophores. In *Principles of Fluorescence Spectroscopy*; Springer US, 2006; bll 63–95.
(48) Lakowicz, J. R.; Piszczek, G.; Kang, J. S. On the Possibility of Long-Wavelength Long-Lifetime High-Quantum-Yield Luminophores. *Anal. Biochem.* **2001**, *288* (1), 62–75.
(49) Maliwal, B. P.; Gryczynski, Z.; Lakowicz, J. R. Long-Wavelength Long-Lifetime Luminophores. *Anal.Chem.* **2001**, *73* (17), 4277–4285.
(50) Kang, J. S.; Piszczek, G.; Lakowicz, J. R. Enhanced Emission Induced by FRET from a Long-Lifetime, Low Quantum Yield Donor to a Long-Wavelength, High Quantum Yield Acceptor. *J. Fluoresc.* **2002**, *12* (1), 97–103.
(51) Gryczynski, Z.; Maliwal, B. P.; Gryczynski, I.; Lakowicz, J. R. Long-Wavelength Long-Lifetime Luminophores for Cellular and Tissue Imaging. In *Proceedings of the Society of Photo-Optical Instrumentation Engineers*; SPIE-INT SOC Optical Engineering: San Jose, CA, 2004; Vol 5323, bll 88–98.
(52) Demchenko, A. P. Sensing Inside the Living Cells. In *Introduction to Fluorescence Sensing*; Springer Netherlands: Dordrecht, 2015; bll 603–675.
(53) Collier, B. B.; McShane, M. J. Time-Resolved Measurements of Luminescence. *J. Lumin.* **2013**, *144*, 180–190.
(54) Kowalska-Baron, A.; Gałęcki, K.; Wysocki, S. Room Temperature Phosphorescence study on the structural flexibility of single tryptophan containing proteins. *Spectrochim. Acta. A. Mol. Biomol. Spectrosc.* **2015**, *134*, 380–387.

(55) Lakowicz, J. R. Time-Domain Lifetime Measurements. In *Principles of Fluorescence Spectroscopy*; Springer US, 2006; bll 96–155.
(56) McGraw, C. M.; Khalil, G.; Callis, J. B. Comparison of Time and Frequency Domain Methods for Luminescence Lifetime Measurements †. *J. Phys. Chem. C* **2008**, *112* (21), 8079–8084.
(57) Lakowicz, J. R.; Gryczynski, I.; Gryczynski, Z.; Johnson, M. L. Background Suppression in Frequency-Domain Fluorometry. *Anal. Biochem.* **2000**, *277* (1), 74–85.
(58) Rowe, H. M.; Chan, S. P.; Demas, J. N.; DeGraff, B. A. Elimination of Fluorescence and Scattering Backgrounds in Luminescence Lifetime Measurements Using Gated-Phase Fluorometry. *Anal. Chem.* **2002**, *74* (18), 4821–4827.
(59) Demchenko, A. P. Fluorescence Detection Techniques. In *Introduction to Fluorescence Sensing*; Springer Netherlands: Dordrecht, 2015; bll 69–132.
(60) Gahlaut, N.; Miller, L. W. Time-Resolved Microscopy for Imaging Lanthanide Luminescence in Living Cells. *Cytometry. A* **2010**, *77* (12), 1113–1125.
(61) Schwartz, P. A.; Murray, B. W. Protein kinase biochemistry and drug discovery. *Bioorg. Chem.* **2011**, *39* (5-6), 192–210.
(62) Manning, G.; Whyte, D. B.; Martinez, R.; Hunter, T.; Sudarsanam, S. The Protein Kinase Complement of the Human Genome. *Science* **2002**, *298* (5600), 1912–1934.
(63) Pearce, L. R.; Komander, D.; Alessi, D. R. The Nuts and Bolts of AGC Protein Kinases. *11* (1).
(64) Cohen, P. Protein Kinases – the Major Drug Targets of the Twenty-First Century? *Nat. Rev. Drug Discov.* **2002**, *1* (April), 309–315.
(65) Goswami, A.; Burikhanov, R.; de Thonel, A.; Fujita, N.; Goswami, M.; Zhao, Y.; Eriksson, J. E.; Tsuruo, T.; Rangnekar, V. M. Binding and Phosphorylation of Par-4 by Akt Is Essential for Cancer Cell Survival. *Mol. Cell* **2005**, *20* (1), 33–44.
(66) Gazarini, M. L.; Beraldo, F. H.; Almeida, F. M.; Bootman, M.; Da Silva, A. M.; Garcia, C. R. S. Melatonin Triggers PKA Activation in the Rodent Malaria Parasite Plasmodium chabaudi. *J. Pineal Res.* **2011**, *50* (1), 64–70.
(67) Uehata, M.; Ishizaki, T.; Satoh, H.; Ono, T.; Kawahara, T.; Morishita, T.; Tamakawa, H.; Yamagami, K.; Inui, J.; Maekawa, M.; et al. Calcium Sensitization of Smooth Muscle Mediated by a Rho-Associated Protein Kinase in Hypertension. *Nature* **1997**, *389* (6654), 990–994.
(68) Skalhegg, Bjorn, S. Specificity in the cAMP/PKA Signaling Pathway. Differential Expression, Regulation, and Subcellular Localization of Subunits of PKA. *Front. Biosci.* **2000**, *5* (1), d678.
(69) Johnson, D. A.; Akamine, P.; Radzio-Andzelm, E.; Taylor, S. S. Dynamics of cAMP-Dependent Protein Kinase. *Chem. Rev.* **2001**, *101* (8), 2243–2270.
(70) Shabb, J. B. Physiological Substrates of cAMP-Dependent Protein Kinase. *Chem. Rev.* **2001**, *101* (8), 2381–2412.
(71) Adams, S. R.; Campbell, R. E.; Gross, L. A.; Martin, B. R.; Walkup, G. K.; Yao, Y.; Llopis, J.; Tsien, R. Y. New Biarsenical Ligands and Tetracysteine Motifs for Protein Labeling in Vitro and in Vivo: Synthesis and Biological Applications. *J. Am. Chem. Soc.* **2002**, *124* (21), 6063–6076.
(72) Jing, C.; Cornish, V. W. Chemical Tags for Labeling Proteins Inside Living Cells. *Acc. Chem. Res.* **2011**, *44* (9), 784–792.

(73) Dyachok, O.; Isakov, Y.; Sågetorp, J.; Tengholm, A. Oscillations of Cyclic AMP in Hormone-Stimulated Insulin-Secreting Beta-Cells. *Nature* **2006**, *439* (7074), 349–352.
(74) Hoffmann, C.; Gaietta, G.; Zürn, A.; Adams, S. R.; Terrillon, S.; Ellisman, M. H.; Tsien, R. Y.; Lohse, M. J. Fluorescent Labeling of Tetracysteine-Tagged Proteins in Intact Cells. *Nat. Protoc.* **2010**, *5* (10), 1666–1677.
(75) Stroffekova, K.; Proenza, C.; Beam, K. The CCXXCC Reagent Flash Binds Non-Specifically to Cellular Cysteine-Rich Proteins. *Biophys. J.* **2000**, *78* (1), 442A – 442A.
(76) Zaccolo, M.; De Giorgi, F.; Cho, C. Y.; Feng, L.; Knapp, T.; Negulescu, P. A.; Taylor, S. S.; Tsien, R. Y.; Pozzan, T. A Genetically Encoded, Fluorescent Indicator for Cyclic AMP in Living Cells. *Nat. Cell Biol.* **2000**, *2* (1), 25–29.
(77) Lissandron, V.; Terrin, A.; Collini, M.; D'alfonso, L.; Chirico, G.; Pantano, S.; Zaccolo, M. Improvement of a FRET-based Indicator for cAMP by Linker Design and Stabilization of Donor-Acceptor Interaction. *J. Mol. Biol.* **2005**, *354* (3), 546–555.
(78) Heim, R.; Tsien, R. Y. Engineering Green Fluorescent Protein for Improved Brightness, Longer Wavelengths and Fluorescence Resonance Energy Transfer. *Curr. Biol.* **1996**, *6* (2), 178–182.
(79) Lim, R. Y. H.; Aebi, U.; Fahrenkrog, B. Towards Reconciling Structure and Function in the Nuclear Pore Complex. *Histochem. Cell Biol.* **2008**, *129* (2), 105–116.
(80) Popken, P.; Ghavami, A.; Onck, P. R.; Poolman, B.; Veenhoff, L. M. Size-Dependent Leak of Soluble and Membrane Proteins Through the Yeast Nuclear Pore Complex. *Mol. Biol. Cell* **2015**, *26* (7), 1386–1394.
(81) Wang, R.; Brattain, M. G. The Maximal Size of Protein to Diffuse Through the Nuclear Pore Is Larger than 60kDa. *FEBS Lett.* **2007**, *581* (17), 3164–3170.
(82) Vaasa, A.; Lust, M.; Terrin, A.; Uri, A.; Zaccolo, M. Small-Molecule FRET Probes for Protein Kinase Activity Monitoring in Living Cells. *Biochem. Biophys. Res. Commun.* **2010**, *397* (4), 750–755.
(83) Higashi, H.; Sato, K.; Ohtake, A.; Omori, A.; Yoshida, S.; Kudo, Y. Imaging of cAMP-Dependent Protein Kinase Activity in Living Neural Cells Using a Novel Fluorescent Substrate. *FEBS Lett.* **1997**, *414* (1), 55–60.
(84) Enkvist, E.; Kriisa, M.; Roben, M.; Kadak, G.; Raidaru, G.; Uri, A. Effect of the Structure of Adenosine Mimic of Bisubstrate-Analog Inhibitors on Their Activity Towards Basophilic Protein Kinases. *Bioorg. Med. Chem. Lett.* **2009**, *19* (21), 6098–6101.
(85) Pflug, A.; Rogozina, J.; Lavogina, D.; Enkvist, E.; Uri, A.; Engh, R. A.; Bossemeyer, D. Diversity of Bisubstrate Binding Modes of Adenosine Analogue-Oligoarginine Conjugates in Protein Kinase a and Implications for Protein Substrate Interactions. *J. Mol. Biol.* **2010**, *403* (1), 66–77.
(86) Vinogradov, S. A.; Fernandez-Searra, M. A.; Dugan, B. W.; Wilson, D. F. Frequency Domain Instrument for Measuring Phosphorescence Lifetime Distributions in Heterogeneous Samples. *Rev. Sci. Instrum.* **2001**, *72* (8), 3396–3406.
(87) Vaasa, A.; Viil, I.; Enkvist, E.; Viht, K.; Raidaru, G.; Lavogina, D.; Uri, A. High-Affinity Bisubstrate Probe for Fluorescence Anisotropy Binding/ Displacement Assays with Protein Kinases PKA and ROCK. *Anal. Biochem.* **2009**, *385* (1), 85–93.

(88) Kagan, M.; Kivirand, K.; Rinken, T. Modulation of Enzyme Catalytic Properties and Biosensor Calibration Parameters with Chlorides: Studies with Glucose Oxidase. *Enzyme Microb. Technol.* **2013**, *53* (4), 278–282.
(89) Morris, J. V.; Mahaney, M. A.; Huber, J. R. Fluorescence Quantum Yield Determinations. 9,10-Diphenylanthracene as a Reference Standard in Different Solvents. *J. Phys. Chem.* **1976**, *80* (9), 969–974.
(90) Kubin, R.; Fletcher, A. Fluorescence Quantum Yields of Some Rhodamine Dyes. *J. Lumin.* **1982**, *27* (4), 455–462.
(91) Lakowicz, J. R. Energy Transfer Efficiency From Enhanced Acceptor Fluorescence. In *Principles of Fluorescence Spectroscopy*; Springer US: Boston, MA, 2006; bll 461–462.
(92) Ligi, K.; Enkvist, E.; Uri, A. Deoxygenation Increases Photoluminescence Lifetime of Protein-Responsive Organic Probes with Triplet–Singlet Resonant Energy Transfer. *J. Phys. Chem. B* **2016**, *120* (22), 4945–4954.
(93) Lavogina, D.; Lust, M.; Viil, I.; König, N.; Raidaru, G.; Rogozina, J.; Enkvist, E.; Uri, A.; Bossemeyer, D. Structural Analysis of ARC-Type Inhibitor (ARC-1034) Binding to Protein Kinase A Catalytic Subunit and Rational Design of Bisubstrate Analogue Inhibitors of Basophilic Protein Kinases. *J. Med. Chem.* **2009**, *52* (2), 308–321.
(94) Butler, S. J.; Delbianco, M.; Lamarque, L.; McMahon, B. K.; Neil, E. R.; Pal, R.; Parker, D.; Walton, J. W.; Zwier, J. M. EuroTracker® Dyes: Design, Synthesis, Structure and Photophysical Properties of Very Bright Europium Complexes and Their Use in Bioassays and Cellular Optical Imaging. *Dalton Trans.* **2015**, *44* (11), 4791–4803.
(95) Kasari, M.; Padrik, P.; Vaasa, A.; Saar, K.; Leppik, K.; Soplepmann, J.; Uri, A. Time-Gated Luminescence Assay Using Nonmetal Probes for Determination of Protein Kinase Activity-Based Disease Markers. *Anal. Biochem.* **2012**, *422* (2), 79–88.
(96) Lavogina, D.; Enkvist, E.; Uri, A. Bisubstrate Inhibitors of Protein Kinases: from Principle to Practical Applications. *ChemMedChem* **2010**, *5* (1), 23–34.
(97) Ekokoski, E.; Aitio, O.; Törnquist, K.; Yli-Kauhaluoma, J.; Tuominen, R. K. HIV-1 Tat-Peptide Inhibits Protein Kinase C and Protein Kinase A Through Substrate Competition. *Eur. J. Pharm. Sci.* **2010**, *40* (5), 404–411.
(98) Ramos-Molina, B.; Lick, A. N.; Nasrolahi Shirazi, A.; Oh, D.; Tiwari, R.; El-Sayed, N. S.; Parang, K.; Lindberg, I.; Joliot, A.; Prochiantz, A.; et al. Cationic Cell-Penetrating Peptides Are Potent Furin Inhibitors. *PLoS One* **2015**, *10* (6), e0130417.
(99) Ziegler, A.; Seelig, J. High Affinity of the Cell-Penetrating Peptide HIV-1 Tat-PTD for DNA. *Biochemistry* **2007**, *46* (27), 8138–8145.
(100) Vermeulen, L.; Berghe, W. Vanden; Beck, I. M. E.; De Bosscher, K.; Haegeman, G. The Versatile Role of MSKs in Transcriptional Regulation. *Trends Biochem. Sci.* **2009**, *34* (6), 311–318.

ACKNOWLEDGMENTS

First and foremost, I would like to express my gratitude to my supervisors Dr. Asko Uri and Dr. Erki Enkvist. I am thankful for Asko for providing me with the opportunity to perform my PhD project under his guidance. In addition, Asko has provided me the opportunity to gain professional experience in great laboratories in different parts of the world, which has been an invaluable experience. Also, this PhD thesis would not have been completed without the professional guidance and moral support from Dr. Erki Enkvist. I appreciate his insight into the scientific problems that were addressed within the current research project and the professional discussions that we have had during my PhD studies.

I am thankful for Prof. L.W. Miller, Dr. L.-O. Pålsson, Prof. S. Vinogradov, and Prof. D. Papkovsky for hosting me at their laboratories. The collaborations have not always been on a smooth road, but all the associates have always given their best to make it worthwhile. I would also like to bring out Dr. R. Pal, Prof. J.A.G. Williams, Dr. S. Mohandessi, Dr. R. Dmitriev, Dr. A. Zhdanov and Dr. T. Esipova for helping me to perform my research project and for showing interest into my well-being while working abroad and thereby making the journey more enjoyable.

I am thankful to all of my co-authors for their professional input into the project. I would like to bring out Dr. Angela Vaasa – it was a great pleasure to work with her.

I have been blessed with great group members that never turn a blind eye to a co-worker. They have been there for me to share my joys as well as my downfalls in the laboratory. My great thanks goes to all of them: Hedi, Marie, Taavi, Jürgen, Kaido, Darja, Marje and Katrin. I wish you all the best with your research and luck in life.

I would also like to bring out Prof. Ago Rinken's research group for their professional support, especially Dr. Olga Mazina and Dr. Sergei Kopanchuk.

Last, but not least, I would like to thank my friends and family, especially Kristjan for his unquestioning belief in me.

CURRICULUM VITAE

Name: Kadri Ligi
Date of Birth: December 26, 1985
Citizenship: Estonian
Addresss: University of Tartu, Institute of Chemistry
Ravila 14a, 50411, Tartu, Estonia
Phone: +372 53 485 924
E-mail: kligi@ut.ee

Language skills: Estonian (mother tongue), English (fluent), Russian (basic), French (basic)

Education

2012– ...	University of Tartu, PhD studies in chemistry
2010–2012	University of Tartu, MSc in chemistry
2006–2010	University of Tartu, BSc (biology as main speciality, chemistry as minor speciality)

Professional Self-Improvement

2011	Department of Chemistry, Durham University, UK (2 months)
2012	Department of Chemistry, University of Illinois at Chicago, USA (2 months)
2013, 2014	Department of Biochemistry and Biophysics, Perelman School of Medicine, University of Pennsylvania, USA (5 + 6 weeks)
2014	Biophysics and Bioanalysis Lab, School of Biochemistry & Cell Biology, University College Cork, Ireland (5 weeks)

Professional Acknowledgement

2013	First Prize, Student Award, Estonian Biochemical Society
2013–2014	Scholarship, World Federation of Scientists (WFS), 1 year

Scientific Publications

(1) Enkvist, E.; Vaasa, A.; Kasari, M.; Kriisa, M.; Ivan, T.; **Ligi, K**.; Raidaru, G.; Uri, A. Protein-Induced Long Lifetime Luminescence of Nonmetal Probes. *ACS Chem. Biol.* **2011**, *6* (10), 1052–1062.

(2) Vaasa, A.; **Ligi, K.**; Mohandessi, S.; Enkvist, E.; Uri, A.; Miller, L. W. Time-Gated Luminescence Microscopy with Responsive Nonmetal Probes for Mapping Activity of Protein Kinases in Living Cells. *Chem. Commun.* **2012**, *48* (68), 8595–8597.

(3) Kasari, M.; **Ligi, K**.; Williams, J. A. G.; Vaasa, A.; Enkvist, E.; Viht, K.; Pålsson, L. O.; Uri, A. Responsive Microsecond-Lifetime Photoluminescent Probes for Analysis of Protein Kinases and Their Inhibitors. *Biochim. Biophys. Acta - Proteins Proteomics* **2013**, *1834* (7), 1330–1335.

(4) Ekambaram, R.; Manoharan, G. babu; Enkvist, E.; **Ligi, K.**; Knapp, S.; Uri, A. PIM Kinase-Responsive Microsecond-Lifetime Photoluminescent Probes Based on Selenium-Containing Heteroaromatic Tricycle. *RSC Adv.* **2015**, *5* (117), 96750–96757.

(5) **Ligi, K.**; Enkvist, E.; Uri, A. Deoxygenation Increases Photoluminescence Lifetime of Protein-Responsive Organic Probes with Triplet–Singlet Resonant Energy Transfer. *J. Phys. Chem. B* **2016**, *120* (22), 4945–4954.

ELULOOKIRJELDUS

Nimi: Kadri Ligi
Sünniaeg ja -koht: 26. detsember 1985, Tartu, Eesti
Kodakondsus: Eesti
Aadress: Tartu Ülikool, keemia instituut
Ravila 14a, 50411, Tartu, Estonia
Telefon: +372 53 485 924
E-mail: kligi@ut.ee

Keelteoskus: eesti keel (emakeel), inglise keel (väga hea kõnes ja kirjas), prantsuse keel (algtasemel), vene keel (algtasemel)

Haridus

2012– ...	Tartu Ülikool, keemia doktoriõpe
2010–2012	Tartu Ülikool, keemia magistriõpe
2006–2010	Tartu Ülikool, bioloogia (põhieriala) ja keemia (kõrvaleriala) bakalaureuseõpe

Erialane enesetäiendus

2011	Department of Chemistry, Durham University, Suurbritannia (2 kuud)
2012	Department of Chemistry, University of Illinois at Chicago, USA (2 kuud)
2013, 2014	Department of Biochemistry and Biophysics, Perelman School of Medicine, University of Pennsylvania, USA (5 + 6 nädalat)
2014	Biophysics and Bioanalysis Lab, School of Biochemistry & Cell Biology, University College Cork, Iirimaa (5 nädalat)

Erialane tunnustus

2013	Esimene Auhind Eesti Biokeemia Seltsi poolt korraldataval iga-aastasel üliõpilaste teaduspublikatsioonide konkursil
2013–2014	World Federation of Scientists (WFS) aastane stipendium

Teaduspublikatsioonid

(1) Enkvist, E.; Vaasa, A.; Kasari, M.; Kriisa, M.; Ivan, T.; **Ligi, K**.; Raidaru, G.; Uri, A. Protein-Induced Long Lifetime Luminescence of Nonmetal Probes. *ACS Chem. Biol.* **2011**, *6* (10), 1052–1062.

(2) Vaasa, A.; **Ligi, K.**; Mohandessi, S.; Enkvist, E.; Uri, A.; Miller, L. W. Time-Gated Luminescence Microscopy with Responsive Nonmetal Probes for Mapping Activity of Protein Kinases in Living Cells. *Chem. Commun.* **2012**, *48* (68), 8595–8597.

(3) Kasari, M.; **Ligi, K**.; Williams, J. A. G.; Vaasa, A.; Enkvist, E.; Viht, K.; Pålsson, L. O.; Uri, A. Responsive Microsecond-Lifetime Photo-

luminescent Probes for Analysis of Protein Kinases and Their Inhibitors. *Biochim. Biophys. Acta - Proteins Proteomics* **2013**, *1834* (7), 1330–1335.

(4) Ekambaram, R.; Manoharan, G. babu; Enkvist, E.; **Ligi, K.**; Knapp, S.; Uri, A. PIM Kinase-Responsive Microsecond-Lifetime Photoluminescent Probes Based on Selenium-Containing Heteroaromatic Tricycle. *RSC Adv.* **2015**, *5* (117), 96750–96757.

(5) **Ligi, K.**; Enkvist, E.; Uri, A. Deoxygenation Increases Photoluminescence Lifetime of Protein-Responsive Organic Probes with Triplet–Singlet Resonant Energy Transfer. *J. Phys. Chem. B* **2016**, *120* (22), 4945–4954.

DISSERTATIONES CHIMICAE UNIVERSITATIS TARTUENSIS

1. **Toomas Tamm.** Quantum-chemical simulation of solvent effects. Tartu, 1993, 110 p.
2. **Peeter Burk.** Theoretical study of gas-phase acid-base equilibria. Tartu, 1994, 96 p.
3. **Victor Lobanov.** Quantitative structure-property relationships in large descriptor spaces. Tartu, 1995, 135 p.
4. **Vahur Mäemets.** The ^{17}O and ^{1}H nuclear magnetic resonance study of H_2O in individual solvents and its charged clusters in aqueous solutions of electrolytes. Tartu, 1997, 140 p.
5. **Andrus Metsala.** Microcanonical rate constant in nonequilibrium distribution of vibrational energy and in restricted intramolecular vibrational energy redistribution on the basis of slater's theory of unimolecular reactions. Tartu, 1997, 150 p.
6. **Uko Maran.** Quantum-mechanical study of potential energy surfaces in different environments. Tartu, 1997, 137 p.
7. **Alar Jänes.** Adsorption of organic compounds on antimony, bismuth and cadmium electrodes. Tartu, 1998, 219 p.
8. **Kaido Tammeveski.** Oxygen electroreduction on thin platinum films and the electrochemical detection of superoxide anion. Tartu, 1998, 139 p.
9. **Ivo Leito.** Studies of Brønsted acid-base equilibria in water and non-aqueous media. Tartu, 1998, 101 p.
10. **Jaan Leis.** Conformational dynamics and equilibria in amides. Tartu, 1998, 131 p.
11. **Toonika Rinken.** The modelling of amperometric biosensors based on oxidoreductases. Tartu, 2000, 108 p.
12. **Dmitri Panov.** Partially solvated Grignard reagents. Tartu, 2000, 64 p.
13. **Kaja Orupõld.** Treatment and analysis of phenolic wastewater with microorganisms. Tartu, 2000, 123 p.
14. **Jüri Ivask.** Ion Chromatographic determination of major anions and cations in polar ice core. Tartu, 2000, 85 p.
15. **Lauri Vares.** Stereoselective Synthesis of Tetrahydrofuran and Tetrahydropyran Derivatives by Use of Asymmetric Horner-Wadsworth-Emmons and Ring Closure Reactions. Tartu, 2000, 184 p.
16. **Martin Lepiku.** Kinetic aspects of dopamine D_2 receptor interactions with specific ligands. Tartu, 2000, 81 p.
17. **Katrin Sak.** Some aspects of ligand specificity of P2Y receptors. Tartu, 2000, 106 p.
18. **Vello Pällin.** The role of solvation in the formation of iotsitch complexes. Tartu, 2001, 95 p.
19. **Katrin Kollist.** Interactions between polycyclic aromatic compounds and humic substances. Tartu, 2001, 93 p.

20. **Ivar Koppel.** Quantum chemical study of acidity of strong and superstrong Brønsted acids. Tartu, 2001, 104 p.
21. **Viljar Pihl.** The study of the substituent and solvent effects on the acidity of OH and CH acids. Tartu, 2001, 132 p.
22. **Natalia Palm.** Specification of the minimum, sufficient and significant set of descriptors for general description of solvent effects. Tartu, 2001, 134 p.
23. **Sulev Sild.** QSPR/QSAR approaches for complex molecular systems. Tartu, 2001, 134 p.
24. **Ruslan Petrukhin.** Industrial applications of the quantitative structure-property relationships. Tartu, 2001, 162 p.
25. **Boris V. Rogovoy.** Synthesis of (benzotriazolyl)carboximidamides and their application in relations with *N*- and *S*-nucleophyles. Tartu, 2002, 84 p.
26. **Koit Herodes.** Solvent effects on UV-vis absorption spectra of some solvatochromic substances in binary solvent mixtures: the preferential solvation model. Tartu, 2002, 102 p.
27. **Anti Perkson.** Synthesis and characterisation of nanostructured carbon. Tartu, 2002, 152 p.
28. **Ivari Kaljurand.** Self-consistent acidity scales of neutral and cationic Brønsted acids in acetonitrile and tetrahydrofuran. Tartu, 2003, 108 p.
29. **Karmen Lust.** Adsorption of anions on bismuth single crystal electrodes. Tartu, 2003, 128 p.
30. **Mare Piirsalu.** Substituent, temperature and solvent effects on the alkaline hydrolysis of substituted phenyl and alkyl esters of benzoic acid. Tartu, 2003, 156 p.
31. **Meeri Sassian.** Reactions of partially solvated Grignard reagents. Tartu, 2003, 78 p.
32. **Tarmo Tamm.** Quantum chemical modelling of polypyrrole. Tartu, 2003. 100 p.
33. **Erik Teinemaa.** The environmental fate of the particulate matter and organic pollutants from an oil shale power plant. Tartu, 2003. 102 p.
34. **Jaana Tammiku-Taul.** Quantum chemical study of the properties of Grignard reagents. Tartu, 2003. 120 p.
35. **Andre Lomaka.** Biomedical applications of predictive computational chemistry. Tartu, 2003. 132 p.
36. **Kostyantyn Kirichenko.** Benzotriazole – Mediated Carbon–Carbon Bond Formation. Tartu, 2003. 132 p.
37. **Gunnar Nurk.** Adsorption kinetics of some organic compounds on bismuth single crystal electrodes. Tartu, 2003, 170 p.
38. **Mati Arulepp.** Electrochemical characteristics of porous carbon materials and electrical double layer capacitors. Tartu, 2003, 196 p.
39. **Dan Cornel Fara.** QSPR modeling of complexation and distribution of organic compounds. Tartu, 2004, 126 p.
40. **Riina Mahlapuu.** Signalling of galanin and amyloid precursor protein through adenylate cyclase. Tartu, 2004, 124 p.

41. **Mihkel Kerikmäe.** Some luminescent materials for dosimetric applications and physical research. Tartu, 2004, 143 p.
42. **Jaanus Kruusma.** Determination of some important trace metal ions in human blood. Tartu, 2004, 115 p.
43. **Urmas Johanson.** Investigations of the electrochemical properties of polypyrrole modified electrodes. Tartu, 2004, 91 p.
44. **Kaido Sillar.** Computational study of the acid sites in zeolite ZSM-5. Tartu, 2004, 80 p.
45. **Aldo Oras.** Kinetic aspects of dATPαS interaction with $P2Y_1$ receptor. Tartu, 2004, 75 p.
46. **Erik Mölder.** Measurement of the oxygen mass transfer through the air-water interface. Tartu, 2005, 73 p.
47. **Thomas Thomberg.** The kinetics of electroreduction of peroxodisulfate anion on cadmium (0001) single crystal electrode. Tartu, 2005, 95 p.
48. **Olavi Loog.** Aspects of condensations of carbonyl compounds and their imine analogues. Tartu, 2005, 83 p.
49. **Siim Salmar.** Effect of ultrasound on ester hydrolysis in aqueous ethanol. Tartu, 2006, 73 p.
50. **Ain Uustare.** Modulation of signal transduction of heptahelical receptors by other receptors and G proteins. Tartu, 2006, 121 p.
51. **Sergei Yurchenko.** Determination of some carcinogenic contaminants in food. Tartu, 2006, 143 p.
52. **Kaido Tämm.** QSPR modeling of some properties of organic compounds. Tartu, 2006, 67 p.
53. **Olga Tšubrik.** New methods in the synthesis of multisubstituted hydrazines. Tartu. 2006, 183 p.
54. **Lilli Sooväli.** Spectrophotometric measurements and their uncertainty in chemical analysis and dissociation constant measurements. Tartu, 2006, 125 p.
55. **Eve Koort.** Uncertainty estimation of potentiometrically measured ph and pK_a values. Tartu, 2006, 139 p.
56. **Sergei Kopanchuk.** Regulation of ligand binding to melanocortin receptor subtypes. Tartu, 2006, 119 p.
57. **Silvar Kallip.** Surface structure of some bismuth and antimony single crystal electrodes. Tartu, 2006, 107 p.
58. **Kristjan Saal.** Surface silanization and its application in biomolecule coupling. Tartu, 2006, 77 p.
59. **Tanel Tätte.** High viscosity $Sn(OBu)_4$ oligomeric concentrates and their applications in technology. Tartu, 2006, 91 p.
60. **Dimitar Atanasov Dobchev**. Robust QSAR methods for the prediction of properties from molecular structure. Tartu, 2006, 118 p.
61. **Hannes Hagu**. Impact of ultrasound on hydrophobic interactions in solutions. Tartu, 2007, 81 p.

62. **Rutha Jäger.** Electroreduction of peroxodisulfate anion on bismuth electrodes. Tartu, 2007, 142 p.
63. **Kaido Viht.** Immobilizable bisubstrate-analogue inhibitors of basophilic protein kinases: development and application in biosensors. Tartu, 2007, 88 p.
64. **Eva-Ingrid Rõõm.** Acid-base equilibria in nonpolar media. Tartu, 2007, 156 p.
65. **Sven Tamp.** DFT study of the cesium cation containing complexes relevant to the cesium cation binding by the humic acids. Tartu, 2007, 102 p.
66. **Jaak Nerut.** Electroreduction of hexacyanoferrate(III) anion on Cadmium (0001) single crystal electrode. Tartu, 2007, 180 p.
67. **Lauri Jalukse.** Measurement uncertainty estimation in amperometric dissolved oxygen concentration measurement. Tartu, 2007, 112 p.
68. **Aime Lust.** Charge state of dopants and ordered clusters formation in CaF_2:Mn and CaF_2:Eu luminophors. Tartu, 2007, 100 p.
69. **Iiris Kahn**. Quantitative Structure-Activity Relationships of environmentally relevant properties. Tartu, 2007, 98 p.
70. **Mari Reinik.** Nitrates, nitrites, N-nitrosamines and polycyclic aromatic hydrocarbons in food: analytical methods, occurrence and dietary intake. Tartu, 2007, 172 p.
71. **Heili Kasuk.** Thermodynamic parameters and adsorption kinetics of organic compounds forming the compact adsorption layer at Bi single crystal electrodes. Tartu, 2007, 212 p.
72. **Erki Enkvist.** Synthesis of adenosine-peptide conjugates for biological applications. Tartu, 2007, 114 p.
73. **Svetoslav Hristov Slavov**. Biomedical applications of the QSAR approach. Tartu, 2007, 146 p.
74. **Eneli Härk.** Electroreduction of complex cations on electrochemically polished Bi(*hkl*) single crystal electrodes. Tartu, 2008, 158 p.
75. **Priit Möller.** Electrochemical characteristics of some cathodes for medium temperature solid oxide fuel cells, synthesized by solid state reaction technique. Tartu, 2008, 90 p.
76. **Signe Viggor.** Impact of biochemical parameters of genetically different pseudomonads at the degradation of phenolic compounds. Tartu, 2008, 122 p.
77. **Ave Sarapuu.** Electrochemical reduction of oxygen on quinone-modified carbon electrodes and on thin films of platinum and gold. Tartu, 2008, 134 p.
78. **Agnes Kütt.** Studies of acid-base equilibria in non-aqueous media. Tartu, 2008, 198 p.
79. **Rouvim Kadis.** Evaluation of measurement uncertainty in analytical chemistry: related concepts and some points of misinterpretation. Tartu, 2008, 118 p.
80. **Valter Reedo.** Elaboration of IVB group metal oxide structures and their possible applications. Tartu, 2008, 98 p.

81. **Aleksei Kuznetsov.** Allosteric effects in reactions catalyzed by the cAMP-dependent protein kinase catalytic subunit. Tartu, 2009, 133 p.
82. **Aleksei Bredihhin.** Use of mono- and polyanions in the synthesis of multisubstituted hydrazine derivatives. Tartu, 2009, 105 p.
83. **Anu Ploom.** Quantitative structure-reactivity analysis in organosilicon chemistry. Tartu, 2009, 99 p.
84. **Argo Vonk.** Determination of adenosine A_{2A}- and dopamine D_1 receptor-specific modulation of adenylate cyclase activity in rat striatum. Tartu, 2009, 129 p.
85. **Indrek Kivi.** Synthesis and electrochemical characterization of porous cathode materials for intermediate temperature solid oxide fuel cells. Tartu, 2009, 177 p.
86. **Jaanus Eskusson.** Synthesis and characterisation of diamond-like carbon thin films prepared by pulsed laser deposition method. Tartu, 2009, 117 p.
87. **Marko Lätt.** Carbide derived microporous carbon and electrical double layer capacitors. Tartu, 2009, 107 p.
88. **Vladimir Stepanov.** Slow conformational changes in dopamine transporter interaction with its ligands. Tartu, 2009, 103 p.
89. **Aleksander Trummal.** Computational Study of Structural and Solvent Effects on Acidities of Some Brønsted Acids. Tartu, 2009, 103 p.
90. **Eerold Vellemäe.** Applications of mischmetal in organic synthesis. Tartu, 2009, 93 p.
91. **Sven Parkel.** Ligand binding to 5-HT_{1A} receptors and its regulation by Mg^{2+} and Mn^{2+}. Tartu, 2010, 99 p.
92. **Signe Vahur.** Expanding the possibilities of ATR-FT-IR spectroscopy in determination of inorganic pigments. Tartu, 2010, 184 p.
93. **Tavo Romann**. Preparation and surface modification of bismuth thin film, porous, and microelectrodes. Tartu, 2010, 155 p.
94. **Nadežda Aleksejeva.** Electrocatalytic reduction of oxygen on carbon nanotube-based nanocomposite materials. Tartu, 2010, 147 p.
95. **Marko Kullapere.** Electrochemical properties of glassy carbon, nickel and gold electrodes modified with aryl groups. Tartu, 2010, 233 p.
96. **Liis Siinor.** Adsorption kinetics of ions at Bi single crystal planes from aqueous electrolyte solutions and room-temperature ionic liquids. Tartu, 2010, 101 p.
97. **Angela Vaasa.** Development of fluorescence-based kinetic and binding assays for characterization of protein kinases and their inhibitors. Tartu 2010, 101 p.
98. **Indrek Tulp.** Multivariate analysis of chemical and biological properties. Tartu 2010, 105 p.
99. **Aare Selberg.** Evaluation of environmental quality in Northern Estonia by the analysis of leachate. Tartu 2010, 117 p.
100. **Darja Lavõgina.** Development of protein kinase inhibitors based on adenosine analogue-oligoarginine conjugates. Tartu 2010, 248 p.

101. **Laura Herm.** Biochemistry of dopamine D_2 receptors and its association with motivated behaviour. Tartu 2010, 156 p.
102. **Terje Raudsepp.** Influence of dopant anions on the electrochemical properties of polypyrrole films. Tartu 2010, 112 p.
103. **Margus Marandi.** Electroformation of Polypyrrole Films: *In-situ* AFM and STM Study. Tartu 2011, 116 p.
104. **Kairi Kivirand.** Diamine oxidase-based biosensors: construction and working principles. Tartu, 2011, 140 p.
105. **Anneli Kruve.** Matrix effects in liquid-chromatography electrospray mass-spectrometry. Tartu, 2011, 156 p.
106. **Gary Urb.** Assessment of environmental impact of oil shale fly ash from PF and CFB combustion. Tartu, 2011, 108 p.
107. **Nikita Oskolkov.** A novel strategy for peptide-mediated cellular delivery and induction of endosomal escape. Tartu, 2011, 106 p.
108. **Dana Martin.** The QSPR/QSAR approach for the prediction of properties of fullerene derivatives. Tartu, 2011, 98 p.
109. **Säde Viirlaid.** Novel glutathione analogues and their antioxidant activity. Tartu, 2011, 106 p.
110. **Ülis Sõukand.** Simultaneous adsorption of Cd^{2+}, Ni^{2+}, and Pb^{2+} on peat. Tartu, 2011, 124 p.
111. **Lauri Lipping.** The acidity of strong and superstrong Brønsted acids, an outreach for the "limits of growth": a quantum chemical study. Tartu, 2011, 124 p.
112. **Heisi Kurig.** Electrical double-layer capacitors based on ionic liquids as electrolytes. Tartu, 2011, 146 p.
113. **Marje Kasari.** Bisubstrate luminescent probes, optical sensors and affinity adsorbents for measurement of active protein kinases in biological samples. Tartu, 2012, 126 p.
114. **Kalev Takkis.** Virtual screening of chemical databases for bioactive molecules. Tartu, 2012, 122 p.
115. **Ksenija Kisseljova**. Synthesis of aza-β^3-amino acid containing peptides and kinetic study of their phosphorylation by protein kinase A. Tartu, 2012, 104 p.
116. **Riin Rebane.** Advanced method development strategy for derivatization LC/ESI/MS. Tartu, 2012, 184 p.
117. **Vladislav Ivaništšev.** Double layer structure and adsorption kinetics of ions at metal electrodes in room temperature ionic liquids. Tartu, 2012, 128 p.
118. **Irja Helm.** High accuracy gravimetric Winkler method for determination of dissolved oxygen. Tartu, 2012, 139 p.
119. **Karin Kipper.** Fluoroalcohols as Components of LC-ESI-MS Eluents: Usage and Applications. Tartu, 2012, 164 p.
120. **Arno Ratas.** Energy storage and transfer in dosimetric luminescent materials. Tartu, 2012, 163 p.

121. **Reet Reinart-Okugbeni**. Assay systems for characterisation of subtype-selective binding and functional activity of ligands on dopamine receptors. Tartu, 2012, 159 p.
122. **Lauri Sikk.** Computational study of the Sonogashira cross-coupling reaction. Tartu, 2012, 81 p.
123. **Karita Raudkivi.** Neurochemical studies on inter-individual differences in affect-related behaviour of the laboratory rat. Tartu, 2012, 161 p.
124. **Indrek Saar.** Design of GalR2 subtype specific ligands: their role in depression-like behavior and feeding regulation. Tartu, 2013, 126 p.
125. **Ann Laheäär.** Electrochemical characterization of alkali metal salt based non-aqueous electrolytes for supercapacitors. Tartu, 2013, 127 p.
126. **Kerli Tõnurist.** Influence of electrospun separator materials properties on electrochemical performance of electrical double-layer capacitors. Tartu, 2013, 147 p.
127. **Kaija Põhako-Esko.** Novel organic and inorganic ionogels: preparation and characterization. Tartu, 2013, 124 p.
128. **Ivar Kruusenberg.** Electroreduction of oxygen on carbon nanomaterial-based catalysts. Tartu, 2013, 191 p.
129. **Sander Piiskop.** Kinetic effects of ultrasound in aqueous acetonitrile solutions. Tartu, 2013, 95 p.
130. **Ilona Faustova**. Regulatory role of L-type pyruvate kinase N-terminal domain. Tartu, 2013, 109 p.
131. **Kadi Tamm.** Synthesis and characterization of the micro-mesoporous anode materials and testing of the medium temperature solid oxide fuel cell single cells. Tartu, 2013, 138 p.
132. **Iva Bozhidarova Stoyanova-Slavova.** Validation of QSAR/QSPR for regulatory purposes. Tartu, 2013, 109 p.
133. **Vitali Grozovski**. Adsorption of organic molecules at single crystal electrodes studied by *in situ* STM method. Tartu, 2014, 146 p.
134. **Santa Veikšina**. Development of assay systems for characterisation of ligand binding properties to melanocortin 4 receptors. Tartu, 2014, 151 p.
135. **Jüri Liiv.** PVDF (polyvinylidene difluoride) as material for active element of twisting-ball displays. Tartu, 2014, 111 p.
136. **Kersti Vaarmets.** Electrochemical and physical characterization of pristine and activated molybdenum carbide-derived carbon electrodes for the oxygen electroreduction reaction. Tartu, 2014, 131 p.
137. **Lauri Tõntson**. Regulation of G-protein subtypes by receptors, guanine nucleotides and Mn^{2+}. Tartu, 2014, 105 p.
138. **Aiko Adamson.** Properties of amine-boranes and phosphorus analogues in the gas phase. Tartu, 2014, 78 p.
139. **Elo Kibena**. Electrochemical grafting of glassy carbon, gold, highly oriented pyrolytic graphite and chemical vapour deposition-grown graphene electrodes by diazonium reduction method. Tartu, 2014, 184 p.

140. **Teemu Näykki.** Novel Tools for Water Quality Monitoring – From Field to Laboratory. Tartu, 2014, 202 p.
141. **Karl Kaupmees.** Acidity and basicity in non-aqueous media: importance of solvent properties and purity. Tartu, 2014, 128 p.
142. **Oleg Lebedev**. Hydrazine polyanions: different strategies in the synthesis of heterocycles. Tartu, 2015, 118 p.
143. **Geven Piir.** Environmental risk assessment of chemicals using QSAR methods. Tartu, 2015, 123 p.
144. **Olga Mazina.** Development and application of the biosensor assay for measurements of cyclic adenosine monophosphate in studies of G protein-coupled receptor signalinga. Tartu, 2015, 116 p.
145. **Sandip Ashokrao Kadam.** Anion receptors: synthesis and accurate binding measurements. Tartu, 2015, 116 p.
146. **Indrek Tallo.** Synthesis and characterization of new micro-mesoporous carbide derived carbon materials for high energy and power density electrical double layer capacitors. Tartu, 2015, 148 p.
147. **Heiki Erikson.** Electrochemical reduction of oxygen on nanostructured palladium and gold catalysts. Tartu, 2015, 204 p.
148. **Erik Anderson.** *In situ* Scanning Tunnelling Microscopy studies of the interfacial structure between Bi(111) electrode and a room temperature ionic liquid. Tartu, 2015, 118 p.
149. **Girinath G. Pillai.** Computational Modelling of Diverse Chemical, Bio-chemical and Biomedical Properties. Tartu, 2015, 140 p.
150. **Piret Pikma.** Interfacial structure and adsorption of organic compounds at Cd(0001) and Sb(111) electrodes from ionic liquid and aqueous electrolytes: an *in situ* STM study. Tartu, 2015, 126 p.
151. **Ganesh babu Manoharan.** Combining chemical and genetic approaches for photoluminescence assays of protein kinases. Tartu, 2016, 126 p.
152. **Carolin Siimenson**. Electrochemical characterization of halide ion adsorption from liquid mixtures at Bi(111) and pyrolytic graphite electrode surface. Tartu, 2016, 110 p.
153. **Asko Laaniste.** Comparison and optimisation of novel mass spectrometry ionisation sources. Tartu, 2016, 156 p.
154. **Hanno Evard.** Estimating limit of detection for mass spectrometric analysis methods. Tartu, 2016, 224 p.